

A peer-reviewed version of this preprint was published in PeerJ on 15 August 2017.

[View the peer-reviewed version](https://peerj.com/articles/3650) (peerj.com/articles/3650), which is the preferred citable publication unless you specifically need to cite this preprint.

Hautier L, Billet G, de Thoisy B, Delsuc F. 2017. Beyond the carapace: skull shape variation and morphological systematics of long-nosed armadillos (genus *Dasypus*) PeerJ 5:e3650 <https://doi.org/10.7717/peerj.3650>

Beyond the carapace: skull shape variation and morphological systematics of long-nosed armadillos (genus *Dasypus*)

Lionel Hautier ^{Corresp., 1,2}, Guillaume Billet ³, Benoit De Thoisy ⁴, Frédéric Delsuc ¹

¹ Institut des Sciences de l'Evolution de Montpellier, Université de Montpellier, Montpellier, France

² Mammal Section, Life Sciences, Vertebrate Division, The Natural History Museum, London, United Kingdom

³ Museum national d'Histoire naturelle, Paris, France

⁴ Institut Pasteur de la Guyane, Cayenne, France

Corresponding Author: Lionel Hautier

Email address: lionel.hautier@umontpellier.fr

Background. The systematics of long-nosed armadillos (genus *Dasypus*) has been mainly based on a handful of external morphological characters and classical measurements. Here, we studied the pattern of morphological variation in the skull of long-nosed armadillos species, with a focus on the systematics of the widely distributed nine-banded armadillo (*D. novemcinctus*). **Methods.** We present the first exhaustive 3D comparison of the skull morphology within the genus *Dasypus*, based on μ CT-scans. We used geometric morphometric approaches to explore the patterns of the intra- and interspecific morphological variation of the skull with regard to several factors such as taxonomy, geography, allometry, and sexual dimorphism. **Results.** We show that the shape and size of the skull vary greatly between *Dasypus* species, with *D. pilosus* representing a clear outlier compared to other long-nosed armadillos. The study of the cranial intraspecific variation in *D. novemcinctus* evidences clear links to the geographic distribution and argue in favour of a revision of past taxonomic delimitations. Our detailed morphometric comparisons detected previously overlooked morphotypes of nine-banded armadillo, especially a very distinctive unit circumscribed to the Guiana Shield. **Discussion.** As our results are congruent with recent molecular data and analyses of the structure of paranasal sinuses, we propose that *D. novemcinctus* should be regarded either as a polytypic species (with three to four subspecies) or as a complex of several distinct species.

1 **Beyond the carapace: skull shape variation and morphological systematics of**
2 **long-nosed armadillos (genus *Dasypus*).**

3

4 Lionel Hautier^{1,2}, Guillaume Billet³, Benoit de Thoisy^{4,5}, and Frédéric Delsuc¹

5

6 ¹Institut des Sciences de l'Evolution, UMR5554, CNRS, IRD, EPHE, Université de Montpellier,
7 Montpellier, France.

8 ²Mammal Section, Life Sciences, Vertebrate Division, The Natural History Museum, Cromwell
9 Road, London SW7 5BD, UK.

10 ³Sorbonne Universités, CR2P, UMR 7207, CNRS, Université Paris 6, Muséum National
11 d'Histoire Naturelle, Paris, France.

12 ⁴Institut Pasteur de la Guyane, Cayenne, French Guiana.

13 ⁵Kwata NGO, BP 972, Cayenne, French Guiana.

14

15

16 **Corresponding Author**

17 Lionel Hautier

18 Email address: lionel.hautier@umontpellier.fr.

19 **Abstract**

20 **Background.** The systematics of long-nosed armadillos (genus *Dasypus*) has been mainly based
21 on a handful of external morphological characters and classical measurements. Here, we studied
22 the pattern of morphological variation in the skull of long-nosed armadillos species, with a focus
23 on the systematics of the widely distributed nine-banded armadillo (*D. novemcinctus*).

24 **Methods.** We present the first exhaustive 3D comparison of the skull morphology within the
25 genus *Dasypus*, based on μ CT-scans. We used geometric morphometric approaches to explore
26 the patterns of the intra- and interspecific morphological variation of the skull with regard to
27 several factors such as taxonomy, geography, allometry, and sexual dimorphism.

28 **Results.** We show that the shape and size of the skull vary greatly between *Dasypus* species,
29 with *D. pilosus* representing a clear outlier compared to other long-nosed armadillos. The study
30 of the cranial intraspecific variation in *D. novemcinctus* evidences clear links to the geographic
31 distribution and argues in favour of a revision of past taxonomic delimitations. Our detailed
32 morphometric comparisons detected previously overlooked morphotypes of nine-banded
33 armadillos, especially a very distinctive unit circumscribed to the Guiana Shield.

34 **Discussion.** As our results are congruent with recent molecular data and analyses of the structure
35 of paranasal sinuses, we propose that *D. novemcinctus* should be regarded either as a polytypic
36 species (with three to four subspecies) or as a complex of several distinct species.

37 **Introduction**

38 With their Pan-American distribution, long-nosed armadillos (genus *Dasypus*) constitute an
39 understudied model for Neotropical biogeography. They are the most taxonomically diverse and
40 widespread extant xenarthrans. The genus *Dasypus* traditionally comprises seven extant species
41 (*D. novemcinctus*, *D. hybridus*, *D. septemcinctus*, *D. kappleri*, *D. pilosus*, *D. mazzai*, and *D.*
42 *sabanicola*; Wetzel, 1985; Wilson & Reeder, 2005; Feijo & Cordeiro-Estrela, 2014) and two
43 extinct ones (*D. bellus* and *D. punctatus*; Castro et al., 2013; Castro, 2015). In spite of being one
44 of the earliest diverging cingulate lineages (Gaudin & Wible, 2006; Delsuc et al., 2012; Gibb et
45 al., 2016), the dasypodid early evolutionary history remains poorly known (Castro, 2015). Only
46 three extinct genera were recognized among the Dasypodini: *Anadasypus* from the middle
47 Miocene of Colombia and late Miocene of Ecuador (Carlini, Vizcaíno & Scillato-Yané, 1997;
48 Carlini et al., 2013), *Pliodasypus* from the late Pliocene of Venezuela (Castro et al., 2014), and
49 *Propraopus* from the middle Pleistocene–early Holocene of South America (Castro et al.,
50 2013a).

51 Aside the widespread nine-banded armadillo (*D. novemcinctus*), all extant long-nosed
52 armadillos are restricted to South America. Some species are sympatric in certain areas resulting
53 in competition and possibly supporting divergent behaviours and morphologies. The nine-banded
54 armadillo is likely to be the most abundant armadillo in tropical forests (Wetzel & Mondolfi,
55 1979; Loughry & Mcdonough, 1998) and has the widest distribution of all extant xenarthran
56 species. Its distribution is thought to cover much of South and Central America and parts of
57 North America and ranges from the south-east United States to North western Argentina and
58 Uruguay (McBee & Baker, 1982). The species ability to disperse quickly, as well as its
59 opportunistic and generalist mode of life, could partly explain this large distribution (Smith &

60 Doughty, 1984; Loughry & Mcdonough, 1998) marked by its rapid historical expansion into the
61 United States (Taulman & Robbins, 2014). Such a wide geographical distribution, combined
62 with early-recognized morphological variations (Peters, 1864; Gray, 1873; Allen, 1911;
63 Lönnberg, 1913; Russell, 1953), raise the possibility that major taxonomic subgroups have been
64 overlooked, be it at the subspecific or even specific level.

65 As its vernacular name implies, the genus *Dasypus* is characterized by a long, slender
66 rostrum, which represents at least more than 55% of the length of the head (Gardner, 2008). The
67 different species are usually distinguished by body and cranial measurements, colour differences,
68 and morphological features of the carapace such as the number of movable bands and scutes
69 across the body and the number and shape of osteodermal foramina (Feijo & Cordeiro-Estrela,
70 2016). The carapace is a hallmark of armadillos, and constitutes such a unique feature for
71 mammals that it has dominated the attention of early and modern anatomists and, as a result,
72 partly jeopardized the classification of the group. Its morphology, chiefly the number of movable
73 bands, has been intensively, if not abusively, used in systematic studies. However, even in the
74 so-called nine-banded armadillo, the number of movable bands can vary from 7 to 10 (Wetzel &
75 Mondolfi, 1979). Yet early on, in his *Systema Naturae* (ed. 10, p. 51), (Linnaeus, 1758) casted
76 doubt on the use of the number of movable bands as a criterion to distinguish *Dasypus* species
77 (*i.e.*, *D. septemcinctus* from *D. novemcinctus*). Since then, a number of authors have raised the
78 question whether such external features could be confidently used for systematic purposes.
79 Wetzel and Mondolfi (1979) argued that “although many scientific names of armadillos are
80 based on the number of movable bands, it is proposed here that for vernacular names we
81 discontinue using this variable characteristic and base names upon unique or more consistent
82 features”. In the early 20th century, Hamlett (1939) made similar observations when focusing on

83 the nine-banded armadillo; he considered as impossible to recognize external variations at a
84 subspecific level and concluded that “cranial characters appear to offer the only promise for
85 subspecific analysis of the species” (Hamlett 1939:335). We decided to take up and further
86 discuss Hamlett’s idea since no large review of the dasypodine cranial variation has been
87 undertaken to date.

88 This study aims to further elucidate the pattern of morphological variation seen in the
89 skull of long-nosed armadillos, with a focus on the nine-banded armadillo. Geometric
90 morphometric data were collected for most *Dasypus* species using μ CT-scans. The main
91 questions asked in the present study were whether different patterns of variation in skull shape
92 can be characterized among and within long-nosed armadillo species, and if those patterns could
93 be linked to factors such as taxonomy, geographical distribution, skull size, or sexual
94 dimorphism. Our ultimate goals are to reconstruct the details of the biogeographic distribution of
95 the widespread nine-banded armadillo at the continental scale and to lay the path for a new
96 integrative taxonomy of long-nosed armadillos. A greater understanding of the morphological
97 diversity and patterns of evolution for long-nosed armadillos is timely to effectively conserve
98 these species and will also serve to deepen our knowledge of their peculiar evolution and biology
99 (Loughry & Mcdonough, 2013).

100

101 **Materials & Methods**

102 ***Biological samples***

103 The material studied came from the collections of the *Muséum national d’Histoire naturelle* in
104 Paris (MNHN, collections *Zoologie et Anatomie comparée, Mammifères et Oiseaux*), the Natural
105 History Museum in London (BMNH), the Naturalis Biodiversity Center in Leiden (NBC), the

106 Royal Ontario Museum in Toronto (ROM), the Louisiana State University in Bâton-Rouge
107 (LSU), the American Museum of Natural History in New York (AMNH), the National Museum
108 of Natural History in Washington (USNM), the *Instituto de Pesquisas Científicas e Tecnológicas*
109 *do Estado do Amapá* in Macapá (IEPA), and the *Muséum d'Histoire naturelle* in Geneva, the
110 KWATA association in Cayenne, and the Personal collection of Pierre Charles-Dominique. We
111 analysed 128 skulls belonging to five *Dasypus* species (see Table S1 for a complete list of
112 specimens): *D. novemcinctus*, *D. hybridus*, *D. septemcinctus*, *D. kappleri*, and *D. pilosus* (no
113 data was available for *D. yepesi*, and *D. sabanicola*). With these data we performed a
114 preliminary assessment of the average amounts of cranial variation at the specific level among
115 different populations of *D. novemcinctus* from French Guiana, Guyana, Suriname, Ecuador,
116 Brazil, Venezuela, Colombia, Costa Rica, Belize, Bolivia, Argentina, Paraguay, Uruguay,
117 Panama, Nicaragua, Honduras, Guatemala, Mexico, Peru, and USA (Table S1). Juvenile,
118 subadult, and adult specimens were considered in order to take into account the effect of age,
119 size and differential growth on the dataset. Several studies (Hensel, 1872; Russell, 1953;
120 Ciancio, Castro & Asher, 2012) showed that long-nosed armadillos possess tooth replacement, as
121 typical for mammals, and that the eruption of permanent teeth occurs relatively late, as observed
122 in afrotherians (Asher & Lehmann, 2008). Accordingly, we used eruption of the teeth, suture
123 closure, and size as criteria to identify adult specimens in our dataset.

124

125 ***Geometric morphometric methods***

126 Due to the limitations of the classical qualitative descriptive approach, geometric morphometrics
127 represents a good complementary technique by which to examine intraspecific shape variation.
128 Digital data of all specimens were acquired using X-ray micro-computed tomography (μ CT) at

129 the University of Montpellier (France), at the Natural History Museum (London, UK), and at the
130 AST-RX platform MNHN (Paris, France). Three-dimensional reconstruction and visualization of
131 the skulls were performed using stacks of digital μ CT images with AVIZO v. 6.1.1 software
132 (Visualization Sciences Group 2009). The mandibles and crania of armadillos were quantified
133 with 10 and 84 anatomical landmarks respectively (Fig. 1 and Tables 1 and 2) using ISE-
134 MeshTools (version 1.3.1; Lebrun, 2014). These landmarks were inspired by previous studies
135 performed on different mammalian taxa (Hautier, Lebrun & Cox, 2012; Hautier et al., 2014).
136 Considering the tendency to the reduction of the number of teeth in *Dasyopus* specimens (Allen,
137 1911), which often lack the last dental locus and thus produce an artificial shortening of the
138 entire tooth row, we decided to place a landmark after the seventh teeth and not at the end of the
139 tooth row as it is usually the norm. Since skulls were often incomplete, the number of landmarks
140 was adjusted to account for the maximal morphological variation in a maximum number of
141 individuals; this number was then different whether we performed analyses considering all
142 *Dasyopus* species (10 and 84 landmarks for the mandible and the cranium respectively) or only *D.*
143 *novemcinctus* (10 and 82 landmarks for the mandible and the cranium respectively).

144 All configurations (sets of landmarks) were superimposed using the Procrustes method of
145 generalized leastsquares superimposition (GLS scaled, translated, and rotated configurations so
146 that the intralandmark distances were minimized) following the methods of Rohlf (1999) and
147 Bookstein (1991). Subsequently, mandibular and cranial forms of each specimen were
148 represented by centroid size S , and by multidimensional shape vector v in linearized Procrustes
149 shape space. Shape variability of the skull and the mandible was analysed by Principal
150 Component Analysis (PCA) of shape (Dryden & Mardia, 1998). Analysis and visualization of
151 patterns of shape variation were performed with the interactive software package

152 MORPHOTOOLS (Specht, 2007; Specht, Lebrun & Zollikofer, 2007; Lebrun, 2008; Lebrun et
153 al., 2010).

154 To account for the potentially confounding effects of size allometry on shape, size-
155 corrected shapes were obtained as follows. In a first step, allometric patterns were obtained via
156 regression of Procrustes coordinates against the logarithm of centroid size, yielding an allometric
157 shape vector (ASV), which characterizes cranial allometric patterns. In a second step, regressions
158 of Procrustes coordinates against the logarithm of centroid size were computed for all species,
159 yielding species-specific allometric shape vectors (ASVs). The ASVs represent directions in
160 shape space that characterize species-specific allometric patterns of shape variation. A common
161 allometric shape vector (ASVc), obtained as the mean of all the ASVs, provided a direction in
162 shape space that minimizes potential divergence in mandibular allometric patterns across species
163 (see Lebrun et al., 2010 for further details concerning this methodology). PCres corresponds to
164 principal components of a PCA performed on shape data corrected for allometry. The same
165 analyses have been performed at the intraspecific level and regressions were then computed
166 between the Procrustes coordinates and the logarithm of centroid size for all subgroups (defined
167 at a country level).

168 Multivariate analyses of variance (MANOVA) were performed on the principal component
169 scores of mandibular and cranial mean shapes (35 first PCs, i.e. 90% of the variance) in order to
170 assess the effects of different factors on mandibular and cranial shape variation: clades (species),
171 sex, and geographic distribution (countries). MANOVAs were performed with Past 2.06 (Hammer,
172 Harper & Ryan, 2001). Linear discriminant analyses (LDA) of shape coordinates were
173 performed on the same number of PCs to assess a potential discrimination of skull morphology
174 in relation to phylogeny (*i.e.*, species) and geography (*i.e.*, countries). When a group included

175 only one individual, this specimen was integrated into the dataset as ungrouped cases. A skull
176 from Panama (USNM 171052) was not complete enough to be considered in these analyses. We
177 then decided to perform similar analyses with a reduced set of landmarks (71 landmarks on the
178 cranium) to enable morphological comparisons with other specimens.

179

180 *Linear measurements*

181 Several linear measurements of the skull of *Dasypus* were calculated directly on 3D coordinates
182 of landmarks (Fig. 2). These measurements were used to compare our results with traditional
183 methods of species delineation.

184

185 **Results**

186 *Interspecific variation of skull shape among long-nosed armadillos*

187 A MANOVA performed on the first 35 PCs (i.e. 90% of the variance) indicates a significant
188 morphological differentiation of the mandibles and crania relative to species delimitations
189 (mandible Wilks' lambda=0.01164, F=4.903, p<0.001; cranium Wilks' lambda=0.0005897,
190 F=11, p<0.001). A multivariate regression of the shape component on size, estimated by the
191 logarithm of centroid size, was highly significant for the skull (mandible Wilks' lambda=0.2709,
192 F=6.637, p<0.001; cranium Wilks' lambda=0.0632, F=30.92, p<0.001). When looking at the
193 allometric shape vectors obtained with the centroid size, we found that size explains 18.99% and
194 25.58% of the variation in the whole mandibular and cranial data sets respectively (S2A and
195 S3A).

196 Morphological differences occur among the mandibles of the five species of *Dasypus*
197 (Fig. 3A). The first two principal components (24.73 % and 16.48% of total shape variation)

198 weakly discriminates *D. pilosus* (negative values) from *D. kappleri* (positive values) while all
199 specimens of *D. novemcinctus*, *D. hybridus*, and *D. septemcinctus* sit in the middle of the graph.
200 These axes separate mandibles having a slender horizontal ramus with an elongated anterior part
201 (located in front of the tooth row) and a short ascending ramus with a short coronoid process
202 anteriorly positioned and vertically oriented from mandibles showing a high horizontal ramus
203 with a short anterior part and a long ascending ramus with an elongated and distally oriented
204 coronoid process. Mandibles of different size are poorly discriminated along the first principal
205 component (Fig. 3B). Once the effect of allometry is removed (S4), no clear morphological
206 differentiation is visible along PCres1. All taxa but *D. pilosus* lay in the positive values of
207 PCres2 therefore the variation in this component is mostly restricted to this latter species.

208 The interspecific differences in the cranium of *Dasypus* are apparent in the morphospace
209 defined by the first two principal components. Except for *D. hybridus* and *D. septemcinctus*, all
210 species are well discriminated in the morphospace defined by the two first principal components
211 (Fig. 4A), which explain 28,4% and 14,6% of the variance respectively. The first principal
212 component unequivocally discriminates *D. hybridus* and *D. septemcinctus* from other species,
213 and negatively correlates with a shortened rostrum and enlarged basicranium and braincase (Fig.
214 4A). *D. pilosus* individuals are well discriminated on the second principal component. On PC2
215 (Fig. 4A), the crania of *D. pilosus* appear narrower with a long snout and smaller braincase
216 (positive values) whereas the crania of *D. novemcinctus*, *D. kappleri*, *D. hybridus*, and *D.*
217 *septemcinctus* are wider with a shorter snout and relatively small braincase (negative values). A
218 regression of the first principal component on the logarithm of the centroid size (Fig. 4B) clearly
219 shows that the five species show different size ranges. The biggest crania are long and display
220 longer and wider snout; whereas the smallest crania are short and wide posteriorly and

221 characterized by a short snout. *D. pilosus* clearly remains an outlier once the size effect is
222 removed (S5), while the other species appear less differentiated in the cranium morphospace.
223 The specific differentiation was checked by performing a discriminant analysis and using a
224 classification phase. The classification methods recovered 100% correct classification of
225 specimens.

226 We also performed the same analyses this time including juvenile specimens (S6) but
227 excluding *D. pilosus* since it represents a clear outlier in the morphospace. All juvenile
228 specimens of *D. novemcinctus* tend to congregate in the negative values of the PC1 and then
229 appear more similar in shape to *D. septemcinctus* and *D. hybridus* than the adults. All juveniles
230 of *D. novemcinctus* and *D. septemcinctus* are located in more negative values of PC1 and more
231 positive values of PC2 relative to the adult individuals of their own species. Such a distribution
232 in the morphospace defined by PC1-2 suggests similar ontogenetic trajectories for the two
233 species.

234

235 ***Intraspecific variation of skull shape in nine-banded armadillos***

236 In specimens for which sex was available (22 females and 32 males for the mandible; 19 females
237 and 34 males for the cranium), a MANOVA shows that there is no sexual dimorphism present in
238 the cranial data (Wilks' lambda=0.2429, F=1.514, p=0.182), so sex is unlikely to be responsible
239 for the variation observed in the cranium of *D. novemcinctus*, while it might partly for the
240 mandible (Wilks' lambda=0.2292, F=2.579, p=0.0110). A multivariate regression of the shape
241 component on size was highly significant (mandible, Wilks' lambda=0.3468, F=3.454, p <0.001;
242 cranium, Wilks' lambda=0.1447, F=8.446, p <0.001). When looking at the allometric shape
243 vectors obtained with the centroid size (S2B and S3B), we found that size explains 14.14% and

244 14.32% of the variation in the whole mandibular and cranial data sets respectively. Shape data
245 corrected for allometry are presented in S7 and S8.

246 A weak intraspecific differentiation (per country) is noticeable on the mandibular
247 morphology (mandible, Wilks' lambda=0.0001404, F=1.523, p <0.001; Fig. 5A). The first
248 principal component (9.87% of total shape variation) weakly discriminates specimens from
249 Brazil, Bolivia, Paraguay, Uruguay (positive values) from other specimens (negative values).
250 This axis separates mandibles characterized by robust and short horizontal ramus and long
251 ascending ramus with a high coronoid, low condylar, and poorly individualized angular
252 processes from mandibles with slender and elongated horizontal ramus and short ascending
253 ramus with low coronoid, high condylar, and well individualized angular processes (Fig. 5A). In
254 terms of shape variation, PC2 (4.745% of total shape variation) separates mandibles that show
255 elongated anterior part of the horizontal ramus, short tooth row, high and distally oriented
256 coronoid process from mandibles having reduced anterior part of the horizontal ramus, an
257 elongated tooth row, and low coronoid process. We observed even less differentiation with shape
258 data corrected for allometry (S7), which indicates that some specimens differ significantly in
259 size. This is confirmed by a regression of the first principal component on the logarithm of the
260 centroid size (Fig. 5B) that shows that the specimens from Brazil, Uruguay, Paraguay, Bolivia,
261 Peru, Ecuador, Costa Rica, and Colombia are usually smaller.

262 A MANOVA was also used to explore if the cranial variation matches the geographical
263 distributions of *D. novemcinctus* (Wilks' lambda=2.97x10⁻⁶, F=2.157, p <0.001). When looking
264 at the cranial morphological variation according to geographic origin (*i.e.*, countries) (Fig. 6),
265 several trends can be observed. PC1, accounting for 22.7% variation, demonstrates a change in
266 how domed the dorsal surface of the skull is and positively correlates with an increase in snout

267 length, a decrease in braincase size, jugals more extended dorsoventrally, and shorter pterygoid
268 processes (Fig. 6A). Specific clusters are recognizable on the first principal component with
269 specimens from Brazil, Paraguay, Venezuela (USNM 406700 from Clarines area, North),
270 Ecuador (BMNH-14-4-25-86 from Gualaquiza, South East), Colombia (AMNH 136252 from
271 Villavicencio area, Centre), Peru, Bolivia, Paraguay, and Uruguay that congregate in the
272 negative values whereas all other specimens lay in the positive values. PC2 is responsible for
273 8.6% of the variance, and describes variation in the size of the posterior part of the rostrum; it
274 also displays variation in length of the posterior part of the palate with an anterior border of the
275 palatine that is well behind the posterior end of the tooth row in positive values. This axis mainly
276 separates specimens from USA, Mexico, Belize, Honduras, Guatemala, and Nicaragua (negative
277 values) from other specimens (positive values). We observed less specific differentiation with
278 shape data corrected for allometry (S8), which shows that the different geographical subgroups
279 differ significantly in size. This is confirmed by a regression of the first principal component to
280 the logarithm of the centroid size (Fig. 7).

281 A Linear Discriminant Analysis (LDA) of shape coordinates was performed in order to
282 take into account the entire morphological variation (*i.e.*, 35 first PCs that represent 90.6% of the
283 variance) and to maximize discrimination among specimens belonging to different countries.
284 Only countries for which we had several specimens could be considered here. Three main
285 regional groups were clearly recovered by the analysis (Fig. 8A): a Northern morphotype, a
286 Southern morphotype, and a group circumscribed to the Guiana Shield (GS). The first group
287 from North and Central America includes specimens from the US, Mexico, Guatemala, and
288 Belize. The South American group gathers specimens from Brazil, Uruguay, Bolivia, Peru,
289 Colombia, and Venezuela. Finally, specimens from French Guiana, Suriname, and Guyana

290 congregate in a last distinctive group. Some specimens from Colombia, Venezuela, and Ecuador
291 do not gather with any of those groups and sit in the middle of the graph defined by the first two
292 discriminant axes; these specimens are however well discriminated on the third and fourth
293 discriminant axes (Fig. 8B) and might constitute a fourth individualized regional group among
294 *D. novemcinctus*, called hereafter the Central morphotype.

295 The discriminant model used to separate the regional groups was checked using a
296 classification phase and then used on under-sampled countries (*i.e.*, when n=1) to assess their
297 affiliation to one of the four abovementioned groups. This classification showed 95% correct
298 classification of specimens (S9). Most regional misclassifications were with specimens coming
299 from the limit of the distribution range of the groups. Two Brazilian specimens from Amapa are
300 put together with the Guianan specimens (S9) and confirmed previous results from the PCA
301 where these two specimens clearly depart from the rest of the Brazilian specimens (Fig. 6A).
302 Three specimens from Venezuela (USNM 406700 from Clarines area, North), Ecuador (BMNH-
303 14-4-25-86 from Gualaquiza, South East), and Colombia (AMNH 136252 from Villavicencio
304 area, Centre) were *a posteriori* classified as close to the Southern morphotype. All these
305 specimens were collected East of the Andes (Fig. 9) and grouped with Brazilian specimens in the
306 PCA analyses. Concerning the countries for which only one specimen was available, the
307 classification analyses gave congruent results with the grouping proposed by the principal
308 component analysis: specimens from Paraguay and Peru were classified as being part of the
309 Southern morphotype while specimens from Nicaragua, Honduras, and Costa Rica were
310 classified as grouping with the Northern morphotype (S9). Using a reduced set of landmarks, the
311 specimen from Panama was attributed to the Central morphotype. When performing these
312 classification methods using the four groups as factors (*i.e.*, Northern, Central, Southern, and

313 Guianan morphotypes; see S10), instead of countries, we retrieved 100% correct classification of
314 specimens.

315 We performed very similar analyses (PCA and LDA, see S11) using linear cranial
316 measurements traditionally used in systematic studies. In all cases, these analyses failed to
317 retrieve a clear-cut discrimination between the four groups defined above.

318

319 **Discussion**

320 *Morphological variation of skull among Dasypus species*

321 Skull ratios are commonly used to compare *Dasypus* species, especially the length of the palate
322 to length of skull (PL/CNL) and length of rostrum to length of skull (RL adj./CNL) (Wetzel,
323 1985). Three subgenera are commonly recognized on this basis: *Cryptophractus* (including *D.*
324 *pilosus*), *Hyperoambon* (including *D. kappleri*), and *Dasypus* (including all remaining species)
325 (Wetzel & Mondolfi, 1979). Our results are largely consistent with findings from previous
326 studies regarding existing differences between *Dasypus* species. Allometry substantially explains
327 cranial differences, with the exception of *D. pilosus* that does not follow the main dasypodine
328 allometric trend (Figs. 3 and 4). The hairy long-nosed armadillo clearly departs from the other
329 four *Dasypus* species in being mainly characterized by a lengthening of the snout and mandible
330 and a small development of the braincase and basicranium. All these characteristics were linked
331 to their unique diet, which might predominantly include ants and termites (Castro et al., 2015).
332 Considering these distinctive morphological features and a specific structure of its osteoderms,
333 Castro et al. (2015) recently proposed to include *D. pilosus* in a different genus, i.e.
334 *Cryptophractus*. However, recent molecular results (Gibb et al., 2016) did not support such a
335 taxonomic reassessment and argued for the conservation of the hairy long-nosed armadillo in the

336 genus *Dasypus*. *D. pilosus* thus likely represents a case of rapid acquisition (*i.e.*, 2.8 Ma as
337 estimated by Gibb et al., 2016) of distinctive morphological traits in line with the shift to a
338 divergent behaviour and ecology.

339 Both molecular and morphological data suggested that *D. kappleri* is broadly separated
340 from the other *Dasypus* species (Wetzel & Mondolfi, 1979; Gibb et al., 2016). Mitogenomic data
341 clearly identified *D. kappleri* as the sister group to all other *Dasypus* species from which it
342 diverged more than 12 million years ago (Gibb et al., 2016) and suggested to place it in the
343 distinct genus *Hyperoambon*, as originally proposed by Wetzel and Mondolfi (1979). We
344 retrieved a significant morphological differentiation with all the specimens of *D. kappleri*
345 congregating in the morphospace and being much larger than the other species. However, the
346 cranial morphology of *D. kappleri* still remains very close to that of *D. novemcinctus* when
347 compared to that of *D. septemcinctus*, *D. hybridus*, and *D. pilosus* (Fig. 4). Recently, Feijo and
348 Cordeiro-Estrela (2016) proposed to recognize three species within *D. kappleri* based on
349 morphological differences of the skull and carapace: *D. kappleri* distributed in the Guiana shield;
350 *D. pastasae* occurring from the eastern Andes of Peru, Ecuador, Colombia, and Venezuela south
351 of the Orinoco River into the western Brazilian Amazon; and finally *D. beniensis* that occurs in
352 the lowlands of the Amazonian Brazil and Bolivia to the south of the Madre de Dios, Madeira,
353 and lower Amazon rivers. We only had access to a limited number of specimens but did not
354 retrieve such a clear geographical segregation in shape (S12A), while we observed a mild
355 differentiation in size with the Guianan *D. kappleri* being usually bigger (S12B).

356 Wetzel and Mondolfi (1979:47) placed *D. septemcinctus*, *D. hybridus*, and *D. sabanicola*
357 in the same subgenus together with *D. novemcinctus*. We observed that *D. hybridus* and *D.*
358 *septemcinctus* group together in the morphospace, but are largely separated from *D.*

359 *novemcinctus*. These two species are usually distinguished by external features, *D. hybridus*
360 showing shorter ears and a longer tail than *D. septemcinctus* (Hamlett, 1939; Wetzel &
361 Mondolfi, 1979). Our morphometrical results showed that *D. hybridus* and *D. septemcinctus*
362 display very similar cranial and mandibular morphologies; they also display several cranial
363 characteristics in common with juvenile specimens of *D. novemcinctus*. Such morphological
364 similarities echo recent molecular findings (Gibb et al., 2016) that showed that mitogenomic
365 sequences of *D. hybridus* are almost identical to those of an Argentinian *D. septemcinctus*
366 (99.3% identity). The two species were considered as valid based on cranial and body
367 measurements (Hamlett, 1939; Wetzel, 1985) despite the fact that they display many external
368 resemblances and have very close geographical distribution. A recent study of their internal
369 cranial sinuses also failed to provide diagnostic characters for the distinction of these two genera
370 (Billet et al., unpublished data). Our samples were very limited for both *D. hybridus* (n=4) and
371 *D. septemcinctus* (n=3), but additional samplings will undoubtedly help to define the systematic
372 status of the two species.

373 We did not have access to the two most recently recognized *Dasypus* species: the
374 Yunga's lesser long-nosed armadillo *D. mazzai* (Yepes, 1933), and the northern long-nosed
375 armadillo *D. sabanicola* (Mondolfi, 1967). The validity of the former was and is still hotly
376 debated (Wetzel & Mondolfi, 1979; Vizcaíno, 1995; Gardner, 2008; Feijo & Cordeiro-Estrela,
377 2014), while the specific status of the latter also remains controversial (Wetzel & Mondolfi,
378 1979; Wetzel, 1985). Cranial morphometric data might provide insightful arguments to discuss
379 the systematic status of the two species.

380

381 ***Morphological systematics and skull shape variation in Dasypus***

382 Relative skull shape has previously been examined for systematics purposes in the genus
383 *Dasypus* but never with a focus on patterns of intraspecific variation. Hamlett (1939) casted
384 doubt on the possibility to identify different subgroups within *D. novemcinctus*, while early
385 workers had already recognized several, either at a specific or at a subspecific level. Peters
386 (1864) described *Dasypus fenestratus* from Costa Rica based on the position of the small and
387 numerous major palatine foramina, some of which are connected to the incisive foramina
388 through a groove, between (not in front of) the anterior teeth, its medially shorter palatine bones,
389 the position of the palatine suture posterior to the end of the tooth row, the position of the
390 lacrimal foramen closer to the orbital rim, as well as one character on the extent of the pelvic
391 shield of the carapace. Gray (1873) tentatively recognized as many as seven species of nine-
392 banded armadillos in South and Central Americas, among which five of them were new: *Tatusia*
393 (= *Dasypus*) *granadiana*, *T. leptorhynchus*, *T. brevirostris*, *T. leptocephala*, and *T. boliviensis*. He
394 also followed Peters (1864) and recognized *T. mexicana* (a variety of *D. novemcinctus* in Peters
395 1864), but decided to ignore *T. fenestratus*. Both Peters (1864) and Gray (1873) used a very
396 small number of specimens and Gray (1873) distinguished all these species based mainly on the
397 morphology of the lacrimal bones and minute morphological variation of the head scutes. Allen
398 (1911) later considered *D. fenestratus* and *D. mexicanus* as synonym taxa of subspecific level
399 (*D. novemcinctus fenestratus* Peters). He also described *D. novemcinctus hoplites* from Grenada,
400 a subspecies that he considered to be distinctly characterized by a shorter tooth row due to the
401 absence of the last tooth locus.

402 From the inspection of a series of specimens from Panama, Costa Rica, and Yucatan,
403 Allen (1911) also distinguished a Central American morphotype. Compared to Brazilian
404 specimens, Allen's Central American armadillo is characterized by short palatine bones that do

405 not reach the level of the most posterior teeth, an obvious inflation of the maxillary region
406 located in front of the lacrimal bone, as well as a lateral margin of the skull that is largely convex
407 at the level of the second or third tooth in ventral view. Based on size differences, Hagmann
408 (1908) described the subspecies *D. n. mexianae*, which he thought was restricted to a small area
409 close to the mouth of the Amazon River. Lönnberg (1913) defined *D. n. aequatorialis* from
410 Ecuador, which McBee and Baker (1982) later proposed to consider as a probable synonym to *T.*
411 *granadiana* Gray 1873. His comparisons were based on morphological characteristics of the
412 carapace, *D. n. aequatorialis* showing differences of the occipital portion of the frontal shield as
413 well as different proportions of the scales of the shoulder and pelvic shields. Later on, Russel
414 (1953) proposed to recognize two subspecies in Mexico: *D. n. davisii* in north-western part of
415 Mexico and *D. n. mexicanus* present in most of the country. Even if it is close morphologically to
416 *D. n. mexicanus*, *D. n. davisii* is much smaller in size and displays a few distinctive features such
417 as small maxillary teeth, a narrow mandible with an angular process posteriorly projected, and
418 differences in suture closure patterns and shape with for instance the parietal-frontal sutures that
419 lies well behind the posterior process of the zygomatic arch (Russell, 1953). Most of these early
420 descriptions, be them at a specific and subspecific level, were based on subtle morphological
421 differences and no proper quantification of the skull variation was undertaken up to now.

422 Our statistical analysis of the skull shape demonstrated that *D. novemcinctus* exhibits a
423 significant level of intraspecific variation, with several clearly identified groups within the nine-
424 banded armadillo. While male nine-banded armadillos tend to be slightly larger than females
425 (McBee & Baker, 1982), our multivariate analyses first suggest the absence of sexual
426 dimorphism in the cranium and a slight sexual dimorphism in the mandible. We also show that
427 allometry is likely to explain a substantial part of the observed morphological variation,

428 including geographically. This echoes early findings by Wetzel and Mondolfi (1979) who
429 already pointed out size gradients between different populations of *D. novemcinctus*. Our
430 morphometric analysis successfully retrieved such a geographical differentiation, both in size
431 and shape. Interestingly, our geometric morphometric analyses permitted to define four discrete
432 phenotypic units. These units display very different cranial characters and occupy very distinct
433 geographical distributions, which are in essence allopatric.

434 Specimens from Brazil, Uruguay, Paraguay, Bolivia, Peru, and from regions of Ecuador,
435 Colombia, and Venezuela located east of the Andes make up most of one group and show a very
436 stable pattern of variation (Fig. 9); they are on average smaller than the three remaining groups.
437 Skulls of this Southern morphotype are clearly distinct by showing smaller and flatter skulls with
438 short frontal sinuses, a narrow snout with short premaxillar bones, a narrow interorbital width, a
439 long and slender jugal part of the zygomatic arch, longer pterygoid processes, and a basicranium
440 aligned with the palate in lateral view (Fig. 6). We found no sign of morphological
441 differentiation of specimens from the mouth of the Amazon River, as implied by the proposed
442 recognition of the subspecies *D. n. mexiana* (Hagmann, 1908). The area covered by the
443 specimens attributed to this morphological unit fully encompasses that of the Amazon basin and
444 seemed to be delimited by the Andes on the western side. As a matter of fact, the single
445 Ecuadorian specimen coming from the eastern side of the Andes appeared to be distinct from
446 most other Ecuadorian specimens, but morphologically close to Brazilian and Bolivian
447 specimens. The same holds true for the Peruvian, Colombian, and Venezuelan specimens
448 collected east of the Andes. The distribution of this group is reminiscent of that of the subspecies
449 *D. novemcinctus novemcinctus* Linnaeus, except for the Guiana Shield area (Gardner, 2008). It
450 also recalls a similar lineage molecularly identified (Arteaga et al., unpublished data) and the

451 Southern morphotype evidenced by the analysis of paranasal spaces (Billet et al., unpublished
452 data). Unfortunately the type specimen of *D. novemcinctus*; which is supposedly housed in the
453 Swedish Museum of Natural History in Stockholm (Lönnerberg, 1913), could not be included in
454 our analyses. The type locality of *Dasypus novemcinctus* Linnaeus is “America meridionali” and
455 is generally thought to be from the eastern coast of Brazil (Allen, 1911).

456 The next differentiated group is represented by individuals originating from the Guiana
457 shield region including French Guiana, Guyana, Suriname, and Amapa in Brazil (Fig. 9). All the
458 specimens belonging to this Guianan morphotype display large dome-shaped skulls that share
459 distinctive morphological features including long frontal sinuses, a wide snout with long
460 premaxillar bones, a large interorbital width, large lacrimal bones, a short and massive jugal part
461 of the zygomatic arch, an anterior border of the palatine located well behind the posterior end of
462 the tooth row, shorter pterygoid processes, and a basicranium situated above the palatal plane
463 (Fig. 6). Studies of paranasal sinuses agree with the distinctness of this group and show that the
464 dome-shaped frontal region of Guianan nine-banded armadillos is occupied by a
465 characteristically inflated pair of frontal sinuses that extend posteriorly to the fronto-parietal
466 suture (Billet et al., unpublished data). No subspecies has ever been recognized or proposed in this
467 part of South America, and such a clear-cut morphological divergence of Guianan specimens of
468 *D. novemcinctus* is here proposed for the first time. These morphometric findings corroborate
469 recent molecular studies, which showed that specimens from French Guiana are very distant
470 from the US populations (Huchon et al., 1999) and represent a distinct branch in the dasypodine
471 mitogenomic tree (Gibb et al., 2016; Arteaga et al., submitted).

472 The distribution of the third recognized morphological group is more limited. It is
473 distributed from the western Andes of Ecuador, Colombia, Panama, and Venezuela to Costa Rica

474 (Fig. 9). This Central morphotype is characterized by high and short skulls having moderately
475 developed frontal sinuses, long premaxillar bones, a narrow interorbital width (larger than
476 Southern specimens but narrower than Guianan specimens), a massive anterior part of the
477 zygomatic arch that is much larger than the posterior part, a short and high jugal part of the
478 zygomatic arch that is largely convex ventrally, an anterior border of the palatine located well
479 behind the posterior end of the tooth row, shorter pterygoid processes, and a basicranium well
480 above the palatal plan (Fig. 6). This distribution roughly corresponds to the combined ranges of
481 two previously described subspecies: *D. n. fenestratus* (Peters, 1864) and *D. n. aequatorialis*
482 (Lönnberg, 1913). These close morphological resemblances suggest that these subspecies might
483 be synonym taxa. However, we could not fully test this hypothesis since we had only access to
484 one specimen from West of the Andes in Peru, Ecuador and southern Bolivia. Studies on the
485 paranasal spaces (Billet et al., unpublished data) failed to recognize such a group, and instead
486 gathered some specimens from these regions with specimens from North and Central America,
487 while others (from the western parts of Colombia, Venezuela and from Panama) were judged
488 impossible to be confidently referred to a given frontal sinus morphotype. In contrast, molecular
489 studies recovered a lineage similar to the group recognized here distributing from the Northern
490 Andes and Central America but expanding to western Mexico (Arteaga et al., unpublished data).

491 The last distinct morphotype occurs from Nicaragua to the Southern part of the US (Fig.
492 9). The range of this Northern morphotype spans the proposed distribution areas of the
493 subspecies *D. n. mexicanus* and *D. n. davisii*, as well as the northernmost part of the distribution
494 range of *D. n. fenestratus*. All the skulls from this area display moderately developed frontal
495 sinuses convergent toward the midline, long premaxillar bones, a narrow interorbital width
496 (larger than Southern specimens but narrower than Guianan specimens), a long and slender jugal

497 part of the zygomatic arch that is largely convex ventrally, an anterior border of the palatine
498 located at the level of the posterior end of the tooth row, shorter pterygoid processes, and a
499 basicranium slightly above the palatal plan (Fig. 6). Contrary to Russel (1953), we did not find
500 major morphological cranial differences between north-western and eastern Mexican
501 populations. Our results thus cast doubts on the validity of the subspecies *D. n. davisi*. The
502 morphological homogeneity in this group is also at odds with the presence of two mitochondrial
503 lineages in Mexico (Arteaga et al., 2012, submitted) but is coherent with the presence of nuclear
504 gene flow between them (Arteaga et al., 2011). Within this Northern group, the invasive US
505 armadillo population derived from two geographical sources: one from Mexico and one from
506 south-central Florida where captive animals were presumably released (Loughry & Mcdonough,
507 2013). For a long time, the exact origin of the Floridian introduced population remained
508 uncertain. All the US specimens used in our analyses were proved to belong to the same
509 Northern morphotype. Echoing the results obtained on six microsatellite loci described by
510 Loughry et al. (2009), we interpret our findings as indicative of a close relationship between the
511 two US populations. The recognition of this Northern unit with individuals ranging from Central
512 to Northern America is also in agreement with their distinctive pattern of paranasal sinuses
513 (Billet et al., unpublished data).

514 The newly recognized subgroups within *D. novemcinctus* prompt questions about the role
515 of ecological factors likely to have influenced their morphological differentiation. Morphological
516 variation in skull morphology as a result of ecological factors has been studied in a number of
517 species over recent years (*e.g.*, Caumul and Polly, 2005; Wroe and Milne, 2007; Hautier et al.,
518 2012). Factors such as temperature, diet and competition may cause phenotypic variation and are
519 likely to explain some morphological differences between the identified groups. These ecological

520 factors vary in relation to geography, and differences in geographical distribution can drive
521 selection for different phenotypes, which may eventually lead to distinctive populations or even
522 new species. Since the four *D. novemcinctus* subgroups are not sympatric in most of their
523 respective natural range, we can hypothesize that environment and/or genetic drift, but not
524 competition, may be responsible for some of the observed intraspecific variation. The Northern
525 Andes constitute a clear geographical barrier, which limited contacts between Northern/Central
526 and Southern populations, and thus has likely played a major role in shaping the morphological
527 differentiation of the long-nosed armadillos. This biogeographical barrier seems to have played a
528 significant role in xenarthrans since it also marks the separation between the two living species
529 of tamanduas with *Tamandua mexicana* in the north and *T. tetradactyla* in the south (Superina,
530 Miranda & Abba, 2010), also within naked-tailed armadillos with *Cabassous centralis* in the
531 north and *C. unicinctus* in the south (Abba & Superina, 2010).

532 The geographical distribution of the divergent populations of *D. novemcinctus* recalls the
533 pattern of morphological differentiation recently proposed for the greater long-nosed armadillo
534 (*D. kappleri*), especially for the Guianan specimens (Feijo & Cordeiro-Estrela, 2016). However,
535 in the nine-banded armadillo, we did not find a clear morphological differentiation within the
536 Amazonian basin as defined on the opposite banks of the Madeira-Madre de Dios rivers (Feijo &
537 Cordeiro-Estrela, 2016), which separate *D. pastasae* from *D. beniensis*. Given the extent of
538 morphological variation reported within *D. kappleri*, Feijo and Cordeiro-Estrela (2016)
539 interpreted their findings as indicative of the fact that this species complex diverged earlier than
540 other *Dasypus* species, which would allow them to accumulate more differences. Such a
541 hypothesis seems difficult to conceive in view of the substantial morphological variation
542 observed among different populations of *D. novemcinctus*, which have diverged more recently

543 (3.7 Ma, Gibb et al., 2016). Feijo and Cordeiro-Estrela (2016) also proposed that such
544 cumulative differences may result from strong environmental selective pressures. The newly
545 discovered morphological diversity within *D. kappleri* and *D. novemcinctus* is likely to represent
546 parallel cases of allopatric differentiation in response to diverging environmental pressures. In
547 both cases, only the future collecting of large-scale genomic nuclear data will allow testing these
548 taxonomic proposals based on morphological data.

549

550 **Conclusions**

551 Intraspecific variations can be the result of adaptation to varying local environmental conditions.
552 We showed that morphometrical comparisons enable detection of previously overlooked
553 morphotypes and yield new insights into factors likely to explain differences between
554 populations inhabiting different areas. Our study of the intraspecific variation of the skull in *D.*
555 *novemcinctus* evidences clear links to the geographic distribution and allows a revision of past
556 taxonomic delimitations. Based on the cranial differences observed, we consider that *D.*
557 *novemcinctus* should be regarded either as a polytypic species (with three to four subspecies) or
558 as a complex of several species. In particular, a new unit of nine-banded armadillos from the
559 Guiana Shield could be detected, which is in agreement with most recent investigations of
560 molecular data and internal anatomy (Arteaga et al., unpublished data; Billet et al., unpublished
561 data). The discovery of divergent populations within *D. novemcinctus* has implications for
562 conservation of the species. In some areas, human activities have led to habitat degradation and
563 fragmentation (Zimbres et al., 2013) or even to habitat loss. These divergent populations may be
564 under threat and may require conservation measures, or at least a close re-examination of their
565 conservation status. If we were to consider them as separate management unit and not as a single

566 species with a large distribution, the threat of endangerment to *D. novemcinctus* would need re-
567 evaluation since it is currently classified globally as ‘Least Concern’ by the IUCN (Loughry,
568 McDonough & Abba, 2014). In addition, our results demonstrate that specimens of *D.*
569 *novemcinctus* should be chosen with caution when making anatomical comparisons or
570 performing cladistic analyses (*e.g.*, Castro et al., 2015); their geographical distribution should be
571 at least specified in all cases. This morphological investigation needs to be extended to the other
572 parts of the body, the carapace in particular. The cranial differences detected among the defined
573 groups might be linked to previously detected differences in the number and shape of scutes on
574 the head shield (*e.g.*, Lönnberg, 1913). Geometric morphometric data holds out the possibility of
575 studying effectively covariation patterns between osteological parts and features of the carapace.
576 Given the quality of the cingulate fossil record, using geometric morphometric methods seems
577 equally conceivable on extinct forms and might also provide fruitful ways to interpret past
578 morphological diversity.

579

580 **Acknowledgements**

581 We are grateful to Christiane Denys, Violaine Nicolas, and Géraldine Véron, (Muséum National
582 d’Histoire Naturelle, Paris), Roberto Portela Miguez, Louise Tomsett and Laura Balcells (British
583 Museum of Natural History, London), Eileen Westwig (American Museum of Natural History,
584 New-York), Burton Lim (Royal Ontario Museum, Toronto), Nicole Edmison and Chris Helgen
585 (National Museum of Natural History, Washington), Jake Esselstyn (Louisiana State University,
586 Baton-Rouge), Manuel Ruedi (*Muséum d’Histoire naturelle*, Geneva), Claudia Regina da Silva
587 (*Instituto de Pesquisas Científicas e Tecnológicas do Estado do Amapá*, Macapá), Steven van
588 der Mije (Naturalis Biodiversity Center, Leiden), François Cazeflis and Suzanne Jiquel (Institut

589 des Sciences de l'Evolution, Montpellier), Lucile Dudoignon (KWATA association), Dominique
590 Charles (CNRS), Maria-Clara Arteaga, Maria Nazareth da Silva (*Instituto de Pesquisas*
591 *Científicas e Tecnológicas do Estado do Amapá*) for access to comparative material. We thank
592 Clara Belfiore for her help in the data acquisition. R. Lebrun (Institut des Sciences de
593 l'Evolution, Montpellier), Farah Ahmed (British Museum of Natural History, London), Miguel
594 García-Sanz and Florent Goussard (Platform AST-RX MNHN) generously provided help and
595 advice on the acquisition of CT scans. Some of the experiments were performed using the μ -CT
596 facilities of the Montpellier Rio Imaging (MRI) platform and of the LabEx CeMEB. This is
597 contribution ISEM 2017-XXX of the Institut des Sciences de l'Evolution.

598

599

600 **Funding**

601 This work has benefited from an "Investissements d'Avenir" grant managed by Agence Nationale
602 de la Recherche, France (CEBA, ref. ANR-10-LABX-25-01). This research received support
603 from the Synthesys Project (<http://synthesys3.myspecies.info/>), which is financed by the
604 European Community Research Infrastructure Action under the FP7.

605

606

607 **Grant Disclosures**

608 The following grant information was disclosed by the authors:

609 Agence Nationale de la Recherche: contract ANR-10-LABX-25-01.

610

611

612 **Competing Interests**

613 The authors declare no competing interests.

614

615

616 **Author Contributions**

617 • Lionel Hautier conceived and designed the experiments, contributed materials, performed the
618 experiments, analysed the data, wrote the paper.

619 • Guillaume Billet conceived and designed the experiments, contributed materials.

620 • Benoit de Thoisy contributed materials.

621 • Frédéric Delsuc conceived and designed the experiments, contributed materials.

622 • All authors read, discussed, corrected, and approved the final version of the paper.

623

624

625 **Data Deposition**

626 The following information was supplied regarding the deposition of related data:

627 Dryad, <http://dx.doi.org/xxxxx>.

628 **References**

- 629 Abba AM., Superina M. 2010. The 2009/2010 armadillo red list assessment. *Edentata* 11:135–
630 184.
- 631 Allen G. 1911. Mammals of the west indies. *Bulletin of the useum of Comparative Zoology*
632 54:175–263.
- 633 Arteaga MC., McCormack JE., Eguiarte LE., Medellín RA. 2011. Genetic admixture in
634 multidimensional environmental space: asymmetrical niche similarity promotes gene flow
635 in armadillos (*Dasypus novemcinctus*). *Evolution* 65:2470–2480.
- 636 Arteaga MC., Piñero D., Eguiarte LE., Gasca J., Medellín R. 2012. Genetic structure and
637 diversity of the nine-banded armadillo in Mexico. *Journal of Mammalogy* 93:547–559.
- 638 Asher RJ., Lehmann T. 2008. Dental eruption in afrotherian mammals. *BMC biology* 6:14. DOI:
639 10.1186/1741-7007-6-14.
- 640 Bookstein F. 1991. *Morphometric tools for landmark data. Geometry and biology*. Cambridge:
641 Cambridge University Press.
- 642 Carlini A a., Castro MC., Madden RH., Scillato-Yané GJ. 2013. A new species of Dasypodidae
643 (Xenarthra: Cingulata) from the late Miocene of northwestern South America: implications
644 in the Dasypodini phylogeny and diversity. *Historical Biology*:37–41. DOI:
645 10.1080/08912963.2013.840832.
- 646 Carlini A., Vizcaíno S., Scillato-Yané G. 1997. Armored xenarthrans: a unique taxonomic and
647 ecologic assemblage. In: Kay R, Madden R, Cifelli R, Flynn J. eds. *Vertebrate paleontology*
648 *in the Neotropics. The Miocene Fauna of La Venta, Colombia*. Washington/London:
649 Smithsonian Institution Press, 213–226.
- 650 Castro MC. 2015. Sistemática y evolución de los armadillos Dasypodini (Xenarthra, Cingulata,

651 Dasypodidae). *Revista del Museo de La Plata* 15:1–50.

652 Castro MC., Avilla LS., Freitas ML., Carlini AA. 2013a. The armadillo *Propraopus sulcatus*
653 (Mammalia: Xenarthra) from the late Quaternary of northern Brazil and a revised synonymy
654 with *Propraopus grandis*. *Quaternary International* 317:80–87. DOI:
655 10.1016/j.quaint.2013.04.032.

656 Castro MC., Carlini A a., Sánchez R., Sánchez-Villagra MR. 2014. A new Dasypodini armadillo
657 (Xenarthra: Cingulata) from San Gregorio Formation, Pliocene of Venezuela: Affinities and
658 biogeographic interpretations. *Naturwissenschaften* 101:77–86. DOI: 10.1007/s00114-013-
659 1131-5.

660 Castro MC., Ciancio MR., Pacheco V., Salas-Gismondi RM., Bostelmann JE., Carlini AA. 2015.
661 Reassessment of the hairy long-nosed armadillo “*Dasypus*”*pilosus* (Xenarthra,
662 Dasypodidae) and revalidation of the genus *Cryptophractus* Fitzinger, 1856. *Zootaxa*
663 3947:30–48. DOI: 10.11646/zootaxa.3947.1.2.

664 Castro MC., Ribeiro AM., Ferigolo J., Langer MC. 2013b. Redescription of *Dasypus punctatus*
665 Lund, 1840 and considerations on the genus *Propraopus* Ameghino, 1881. *Journal of*
666 *Vertebrate Paleontology* 33:434–447. DOI: 10.1080/02724634.2013.729961.

667 Caumul R., Polly P. 2005. Phylogenetic and environmental components of morphological
668 variation: skull, mandible, and molar shape in marmots (*Marmota*, Rodentia). *Evolution*
669 59:2460–2472.

670 Ciancio MR., Castro MC., Asher RJ. 2012. Evolutionary implications of dental eruption in
671 *Dasypus* (Xenarthra). *Journal of Mammalian Evolution* 19:1–8. DOI: 10.1007/s10914-011-
672 9177-7.

673 Delsuc F., Superina M., Tilak M., Douzery EJP., Hassanin A. 2012. Molecular Phylogenetics

674 and Evolution Molecular phylogenetics unveils the ancient evolutionary origins of the
675 enigmatic fairy armadillos. *Molecular Phylogenetics and Evolution* 62:673–680. DOI:
676 10.1016/j.ympev.2011.11.008.

677 Dryden I., Mardia K. 1998. *Statistical shape analysis*. Chichester: John Wiley & Sons.

678 Feijo A., Cordeiro-Estrela P. 2014. The correct name of the endemic *Dasypus* (Cingulata:
679 Dasypodidae) from northwestern Argentina. *Zootaxa* 3887:88–94. DOI:
680 10.11646/zootaxa.3887.1.6.

681 Feijo A., Cordeiro-Estrela P. 2016. Taxonomic revision of the *Dasypus kappleri* complex, with
682 revalidations of *Dasypus pastasae* (Thomas, 1901) and *Dasypus beniensis* Lönnberg, 1942
683 (Cingulata, Dasypodidae). *Zootaxa* 4170:271–297. DOI: 10.11646/zootaxa.4170.2.3.

684 Gardner AF. 2008. *Mammals of South America Volume 1 Marsupials, Xenarthrans, Shrews, and*
685 *Bats*. Chicago and London: The University of Chicago Press.

686 Gaudin TJ., Wible JR. 2006. The Phylogeny of Living and Extinct Armadillos (Mammalia,
687 Xenarthra, Cingulata): A Craniodental Analysis. In: Carrano M, Gaudin TJ, Blob R, Wible
688 JR eds. *Amniote Paleobiology: Perspectives on the Evolution of Mammals, Birds and*
689 *Reptiles*. Chicago: The University of Chicago Press, 153–198.

690 Gibb GC., Condamine FL., Kuch M., Enk J., Moraes-Barros N., Superina M., Poinar HN.,
691 Delsuc F. 2016. Shotgun mitogenomics provides a reference phylogenetic framework and
692 timescale for living xenarthrans. *Molecular Biology and Evolution* 33:621–642. DOI:
693 10.1093/molbev/msv250.

694 Gray J. 1873. *Handlist of the edentate, thick-skinned, and ruminant mammals of the British*
695 *Museum*. London: British Museum of Natural History.

696 Haggmann G. 1908. Die Landsäugetiere der insel Mexiana. Als Beispiel der Einwirkung der

697 isolation auf die umbildung der arten. *Arch. Rass.-Gesell.-Biol. München* 5:1–32.

698 Hamlett G. 1939. Identity of *Dasyopus septemcinctus* Linnaeus with notes on some related
699 species. *Journal of Mammalogy* 20:328–336.

700 Hammer Ø., Harper D., Ryan P. 2001. PAST: paleontological statistics software package for
701 education and data analysis. *Paeontologica Electronica* 4:9.

702 Hautier L., Billet G., Eastwood B., Lane J. 2014. Patterns of Morphological Variation of Extant
703 Sloth Skulls and their Implication for Future Conservation Efforts. *Anatomical Record*
704 297:979–1008. DOI: 10.1002/ar.22916.

705 Hautier L., Lebrun R., Cox PG. 2012. Patterns of covariation in the masticatory apparatus of
706 hystricognathous rodents: implications for evolution and diversification. *Journal of*
707 *morphology* 273:1319–37. DOI: 10.1002/jmor.20061.

708 Hensel R. 1872. *Beiträge zur Kenntnis der Säugethiere Süd-Brasiliens*. Berlin: lis den
709 Abhandlungen der Königl. Akademie der Wissenschaften.

710 Huchon D., Delsuc F., Catzeflis F., Douzery EJP. 1999. Armadillos exhibit less genetic
711 polymorphism in North America than in South America: nuclear and mitochondrial data
712 confirm founder effect in *Dasyopus novemcinctus* (Xenarthra). *Molecular Ecology* 8:1743–
713 1748.

714 Lebrun R. 2008. Evolution and development of the strepsirrhine primate skull. University
715 Montpellier II and University of Zürich.

716 Lebrun R. 2014. ISE-MeshTools, a 3D interactive fossil reconstruction freeware. In: *12th Annual*
717 *Meeting of EAVP*. Torino,.

718 Lebrun R., Ponce de León M., Tafforeau P., Zollikofer C. 2010. Deep evolutionary roots of
719 strepsirrhine primate labyrinthine morphology. *Journal of Anatomy* 216:368–380.

720 Linnaeus C. 1758. *Systema Naturae, Ed; 10. L.* Uppsala: Salvii.

721 Lönnberg E. 1913. Mammals from Ecuador and related forms. *Arkiv för Zoologi* 8:1–36.

722 Loughry WJ., McDonough CM. 1998. Comparisons between nine-banded armadillo (*Dasyopus*
723 *novemcinctus*) populations in Brazil and the United States. *Revista de biología tropical*
724 46:1173–1183.

725 Loughry WJ., McDonough CM. 2013. *The nine-banded armadillo: a natural history*. Norman:
726 University of Oklahoma Press.

727 Loughry J., McDonough C., Abba A. 2014. *Dasyopus novemcinctus*. *The IUCN Red List of*
728 *Threatened Species* 2014:e.T6290A47440785.

729 Loughry WJ., Truman RW., McDonough CM., Tilak M-K., Garnier S., Delsuc F. 2009. Is
730 leprosy spreading among nine-banded armadillos in the southeastern United States? *Journal*
731 *of Wildlife Diseases* 45:144–152. DOI: 10.7589/0090-3558-45.1.144.

732 McBee K., Baker RJ. 1982. *Dasyopus novemcinctus*. *Mammalian Species* 162:1–9.

733 Mondolfi E. 1967. Descripción de un nuevo armadillo del género *Dasyopus* de Venezuela
734 (Mammalia-Edentata). *Memorias de la Sociedad de Ciencias Naturales La Salle* 78:149–
735 167.

736 Peters W. 1864. Über neue Arten de Säugethier-gattungen *Geomys*, *Haplodon* und *Dasyopus*.
737 *Monatsbericht der Königlich- Preussischen Akademie der Wissenschaften zu Berlin*
738 1865:177–181.

739 Rohlf F. 1999. Shape statistics: Procrustes superimpositions and tangent spaces. *Journal of*
740 *Classification* 16:197–223.

741 Russell R. 1953. Description of a new armadillo (*Dasyopus novemcinctus*) from Mexico with
742 remarks on geographic variation of the species. *Proceedings of the Biological Society of*

743 *Washington* 66:21–26.

744 Smith L., Doughty R. 1984. The amazing armadillo: geography of a folk critter. In: Austin:
745 University of Texas Press, 134.

746 Specht M. 2007. Spherical surface parameterization and its application to geometric
747 morphometric analysis of the braincase. University of Zürich Irchel.

748 Specht M., Lebrun R., Zollikofer C. 2007. Visualizing shape transformation between
749 chimpanzee and human braincases. *The Visual Computer* 23:743–751.

750 Superina M., Miranda FR., Abba AM. 2010. The 2010 anteater red list assessment. *Edentata*
751 11:96–114.

752 Taulman JF., Robbins LW. 2014. Range expansion and distributional limits of the nine-banded
753 armadillo in the United States: an update of Taulman & Robbins (1996). *Journal of*
754 *Biogeography* 41:1626–1630.

755 Vizcaíno SF. 1995. Identificación específica de las "mulitas", género *Dasyopus* L. (Mammalia;
756 *Dasyopodidae*); del noroeste argentino. Descripción de una nueva especie. *Mastozoología*
757 *Neotropical* 2:5–13.

758 Wetzel R. 1985. Taxonomy and distribution of armadillos. In: *The Evolution and Ecology of*
759 *Armadillos, Sloths, and Vermilinguas*. Washington DC: Smithsonian Institution Press, 23–
760 46.

761 Wetzel R., Mondolfi E. 1979. The subgenera and species of long-nosed armadillos, genus
762 *Dasyopus*. In: Eisenberg J ed. *Vertebrate Ecology in the Northern Neotropic*. Washington
763 DC: Smithsonian Institution Press, 43–63.

764 Wilson D., Reeder D. 2005. *Mammal species of the world: a taxonomic and geographic*
765 *reference. 3rd ed.* Baltimore: Johns Hopkins University Press.

766 Wroe S., Milne N. 2007. Convergence and remarkably consistent constraint in the evolution of
767 carnivore skull shape. *Evolution* 61:1251–1260.

768 Yepes J. 1933. Una especie nueva de “mulita” (Dasypodinae) para el norte argentino. *Physis*
769 11:225–232.

770 Zimbres B., Furtado MM., Jácomo, Anah T. A. Silveira L., Sollmann R., Tôrres NM., Machado
771 RB., Marinho-Filho J. 2013. The impact of habitat fragmentation on the ecology of
772 xenarthrans (Mammalia) in the Brazilian Cerrado. *Landscape Ecology* 28:259–269.

773

774

775

776 **Table legends**

777 **Table 1.** Definitions of the landmarks used on the mandible.

778

779 **Table 2.** Definitions of the landmarks used on the cranium. Landmarks indicated with a star
780 were not used in the intraspecific comparisons.

781 **Figure Legends**

782

783 **Figure 1.** Landmarks digitized on the mandible and the skull. Dorsal (A), lateral (B), and ventral
784 views of the cranium; medial (C) and lateral (D) views of the mandible.

785

786 **Figure 2.** Illustration of the skull linear measurements. In blue, traditional measurements used in
787 Wetzel (1985). *Abbreviations:* LTC, length between the anterior tip of the nasal and the
788 posteriormost point of the supraoccipital; LR, rostral length; IOB, interorbital breadth; ILFB,
789 inter lacrimal foramina breadth; BB, distance between the left and right intersections between the
790 frontal, parietal, and squamosal sutures; NB, nasal breadth; NL, nasal length; LCB, length
791 between the anterior tip of the premaxillar and the condyles; TL, length of the tooth row; PB,
792 palate breadth; BZP, distance between the infraorbital and the maxillary foramina; MB, inter-
793 meatus breadth; OCB, breadth between the lateral border of the occipital condyle.

794

795 **Figure 3.** (A) Principal component analysis (PC1 vs PC2) and associate patterns of
796 morphological transformation for the mandible of five *Dasypus* species. (B) Regression of the
797 first principal component on the logarithm of the centroid size ($R^2=0.23$; $p<0.001$). *Symbols:*
798 blue squares, *D. kappleri*; black crosses, *D. novemcinctus*; green triangles, *D. hybridus*; green
799 diamonds, *D. septemcinctus*; red circles, *D. pilosus*.

800

801 **Figure 4.** (A) Principal component analysis (PC1 vs PC2) and associate patterns of
802 morphological transformation for crania of five *Dasypus* species. (B) Regression of the first
803 principal component on the logarithm of the centroid size ($R^2=0.55$; $p<0.001$). *Symbols:* blue

804 squares, *D. kappleri*; black crosses, *D. novemcinctus*; green triangles, *D. hybridus*; green
805 diamonds, *D. septemcinctus*; red circles, *D. pilosus*.

806

807 **Figure 5.** (A) Principal component analysis (PC1 vs PC2) and associate patterns of
808 morphological transformation for mandibles of *Dasypus novemcinctus*. (B) Regression of the
809 first principal component on the logarithm of the centroid size ($R^2=0,035$; $p=0.03$). *Symbols:*
810 green diamonds, Bolivia; green triangle, Brazil (solid green triangles are for specimens from
811 Amapa); green circles, Paraguay; green crosses, Peru; green squares, Uruguay; green bars,
812 Venezuela; blue diamonds, Belize; blue “plus”, Guatemala; blue bars, Honduras; Blue squares,
813 Mexico; blue crosses, Nicaragua; blue triangles, USA; blue circles, Costa Rica; black triangles,
814 Colombia; black crosses, Ecuador; black stars, Panama; orange squares, French Guiana; orange
815 crosses, Guyana; orange circles, Suriname.

816

817 **Figure 6.** Principal component analysis (A, PC1 vs PC2; B, PC3 vs PC4) and associate patterns
818 of morphological transformation for crania of *Dasypus novemcinctus*. *Symbols:* green diamonds,
819 Bolivia; green triangle, Brazil (solid green triangles are for specimens from Amapa); green
820 circles, Paraguay; green crosses, Peru; green squares, Uruguay; green bars, Venezuela; blue
821 diamonds, Belize; blue “plus”, Guatemala; blue bars, Honduras; Blue squares, Mexico; blue
822 crosses, Nicaragua; blue triangles, USA; blue circles, Costa Rica; black triangles, Colombia;
823 black crosses, Ecuador; orange squares, French Guiana; orange crosses, Guyana; orange circles,
824 Suriname.

825

826 **Figure 7.** Regression of the first cranial principal component (*Dasypus novemcinctus*) on the

827 logarithm of the centroid size ($R^2=0.15$; $p<0.001$). *Symbols*: green diamonds, Bolivia; green
828 triangle, Brazil (solid green triangles are for specimens from Amapa); green circles, Paraguay;
829 green crosses, Peru; green squares, Uruguay; green bars, Venezuela; blue diamonds, Belize; blue
830 “plus”, Guatemala; blue bars, Honduras; Blue squares, Mexico; blue crosses, Nicaragua; blue
831 triangles, USA; blue circles, Costa Rica; black triangles, Colombia; black crosses, Ecuador;
832 orange squares, French Guiana; orange crosses, Guyana; orange circles, Suriname.

833

834 **Figure 8.** Linear Discriminant Analysis (LDA) performed on cranial shape coordinates of
835 *Dasypus novemcinctus*. *Symbols*: green diamonds, Bolivia; green triangle, Brazil (solid green
836 triangles are for specimens from Amapa); green circles, Paraguay; green crosses, Peru; green
837 squares, Uruguay; green bars, Venezuela; blue diamonds, Belize; blue “plus”, Guatemala; blue
838 bars, Honduras; Blue squares, Mexico; blue crosses, Nicaragua; blue triangles, USA; black
839 triangles, Colombia; black circles, Costa Rica; black crosses, Ecuador; orange squares, French
840 Guiana; orange crosses, Guyana; orange circles, Suriname.

841

842 **Figure 9.** Summary map showing the geographical distribution of nine-banded armadillo
843 specimens investigated in this study and their attribution to one of the four main morphotypes
844 defined in this study: black, Central group; blue, Northern group; green, Southern group; orange,
845 Guianan group. Specimens lacking precise geographical information (other than country of
846 origin) are indicated with a square.

847 **Supplemental Information**

848

849 **S1.** List of measured specimens (used for linear measurements and/or geometric morphometric
850 analyses). *Abbreviations:* MNHN, *Muséum national d'Histoire naturelle* in Paris (collections
851 *Zoologie et Anatomie comparée, Mammifères et Oiseaux*); BMNH, Natural History Museum in
852 London; NBC, Naturalis Biodiversity Center in Leiden; ROM, Royal Ontario Museum in
853 Toronto; LSU, Louisiana State University in Baton-Rouge; AMNH, American Museum of
854 Natural History in New York; USNM, National Museum of Natural History in Washington;
855 IEPA, *Instituto de Pesquisas Científicas e Tecnológicas do Estado do Amapá* in Macapá;
856 MHNG, *Muséum d'Histoire naturelle* in Geneva; KWATA, KWATA association; and PCDPC,
857 Personal collection of Pierre Charles-Dominique.

858

859 **S2.** Regression of the common allometric shape vector (ASVc) on the logarithm of the centroid
860 size for mandibles of five *Dasypus* species (A, $R^2=0.50$; $p<0.001$) and *D. novemcinctus* (B,
861 $R^2=0.34$; $p<0.001$). Below, associate patterns of morphological transformation for mandibles
862 with small (left) and large (right) centroid size. *Symbols:* same as in Figure 3 and 5.

863

864 **S3.** Regression of the common allometric shape vector (ASVc) on the logarithm of the centroid
865 size for crania of five *Dasypus* species (A, $R^2=0.72$; $p<0.001$) and *D. novemcinctus* (B, $R^2=0.48$;
866 $p<0.001$). Below, associate patterns of morphological transformation for crania with small (left)
867 and large (right) centroid size. *Symbols:* same as in Figure 3 and 5.

868

869 **S4.** Principal component analyses with shape data corrected for allometry (PCres1 vs PCres 2)

870 and associate patterns of morphological transformation for mandible of five *Dasyopus* species.
871 *Symbols*: blue squares, *D. kappleri*; black crosses, *D. novemcinctus*; green triangles, *D. hybridus*;
872 green diamonds, *D. septemcinctus*; red circles, *D. pilosus*.

873

874 **S5.** Principal component analyses with shape data corrected for allometry (PCres1 vs PCres 2)

875 and associate patterns of morphological transformation for crania of five *Dasyopus* species.

876 *Symbols*: blue squares, *D. kappleri*; black crosses, *D. novemcinctus*; green triangles, *D. hybridus*;
877 green diamonds, *D. septemcinctus*; red circles, *D. pilosus*.

878

879 **S6. (A)** Principal component analysis (PC1 vs PC2) and associate patterns of morphological

880 transformation for crania of five *Dasyopus* species, including juveniles (indicated with smaller

881 symbols) and excluding *D. pilosus*. **(B)** Regression of the first principal component on the

882 logarithm of the centroid size ($R^2=0,63$; $p<0.001$). *Symbols*: blue squares, *D. kappleri*; black

883 crosses, *D. novemcinctus*; green triangles, *D. hybridus*; green diamonds, *D. septemcinctus*.

884

885 **S7.** Principal component analyses with shape data corrected for allometry (PCres1 vs PCres 2)

886 and associate patterns of morphological transformation for mandibles of *Dasyopus specimens*.

887 *Symbols*: green diamonds, Bolivia; green triangle, Brazil (solid green triangles are for specimens

888 from Amapa); green circles, Paraguay; green crosses, Peru; green squares, Uruguay; green bars,

889 Venezuela; blue diamonds, Belize; blue “plus”, Guatemala; blue bars, Honduras; Blue squares,

890 Mexico; blue crosses, Nicaragua; blue triangles, USA; blue circles, Costa Rica; black triangles,

891 Colombia; black crosses, Ecuador; black stars, Panama; orange squares, French Guiana; orange

892 crosses, Guyana; orange circles, Suriname.

893

894 **S8.** Principal component analyses with shape data corrected for allometry (PCres1 vs PCres 2)

895 and associate patterns of morphological transformation for crania of *Dasypus specimens*.

896 *Symbols:* green diamonds, Bolivia; green triangle, Brazil (solid green triangles are for specimens

897 from Amapa); green circles, Paraguay; green crosses, Peru; green squares, Uruguay; green bars,

898 Venezuela; blue diamonds, Belize; blue “plus”, Guatemala; blue bars, Honduras; Blue squares,

899 Mexico; blue crosses, Nicaragua; blue triangles, USA; blue circles, Costa Rica; black triangles,

900 Colombia; black crosses, Ecuador; orange squares, French Guiana; orange crosses, Guyana;

901 orange circles, Suriname.

902

903 **S9.** Results of *a posteriori* classifications for the discriminant analysis performed on the cranial

904 shape coordinates of *Dasypus novemcinctus* using countries as factors. Specimens with a star (*)

905 were integrated into the analyses as ungrouped cases.

906

907 **S10.** Results of *a posteriori* classifications for the discriminant analysis performed on the cranial

908 shape coordinates of *Dasypus novemcinctus* using the four subgroups (*i.e.*, Northern, Central,

909 Southern, and Guianan morphotypes) as factors. Specimens with a star (*) were integrated into

910 the analyses as ungrouped cases.

911

912 **S11. (A)** Principal component analysis (PC1 vs PC2) and associate patterns of morphological

913 transformation for crania of *Dasypus kappleri*. **(B)** Regression of the first principal component

914 on the logarithm of the centroid size ($R^2=0.40$; $p<0.001$). *Symbols:* green crosses, Peru; green

915 bars, Venezuela; black triangles, Colombia; black crosses, Ecuador; orange squares, French

916 Guiana; orange crosses, Guyana; orange circles, Suriname.

Figure 1

Figure 1

Landmarks digitized on the mandible and the skull. Dorsal (A), lateral (B), and ventral views of the cranium; medial (C) and lateral (D) views of the mandible.

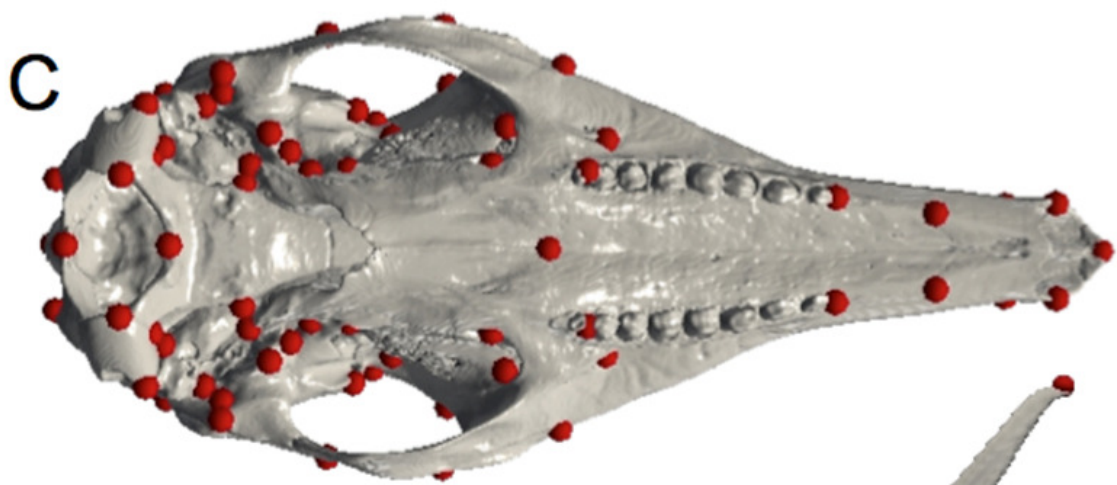
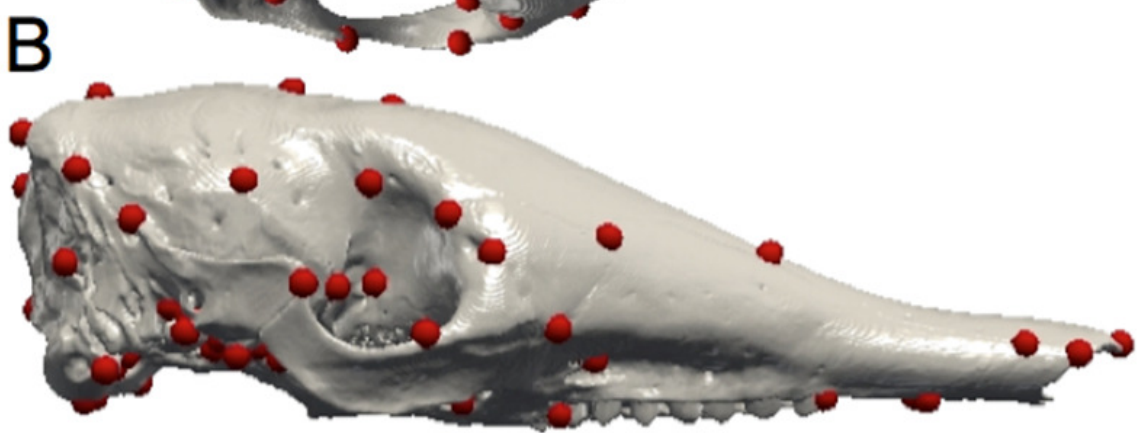
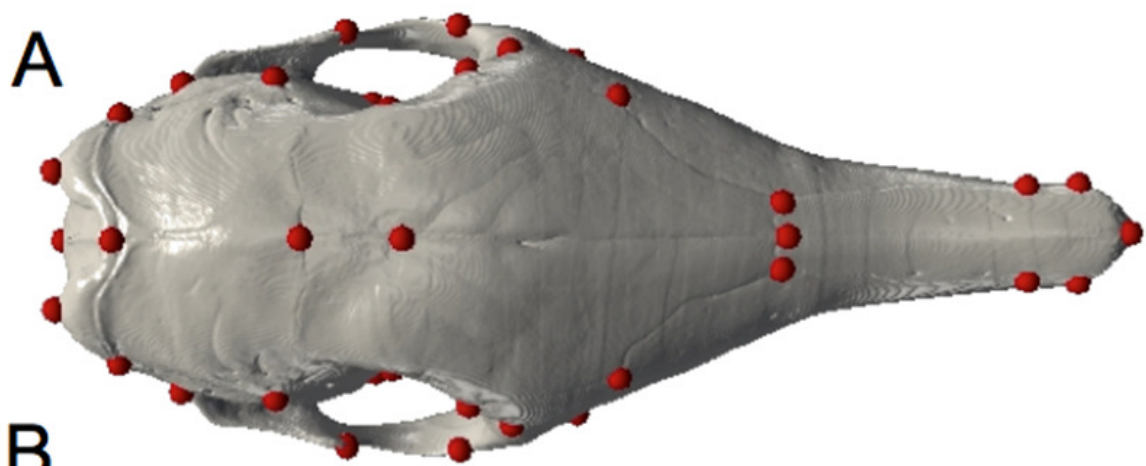


Figure 2

Figure 2

Illustration of the skull linear measurements. In blue, traditional measurements used in Wetzel (1985) . *Abbreviations:* LTC, length between the anterior tip of the nasal and the posteriormost point of the supraoccipital; LR, rostral length; IOB, interorbital breadth; ILFB, inter lacrimal foramina breadth; BB, distance between the left and right intersections between the frontal, parietal, and squamosal sutures; NB, nasal breadth; NL, nasal length; LCB, length between the anterior tip of the premaxillar and the condyles; TL, length of the tooth row; PB, palate breadth; BZP, distance between the infraorbital and the maxillary foramina; MB, inter-meatus breadth; OCB, breadth between the lateral border of the occipital condyle.

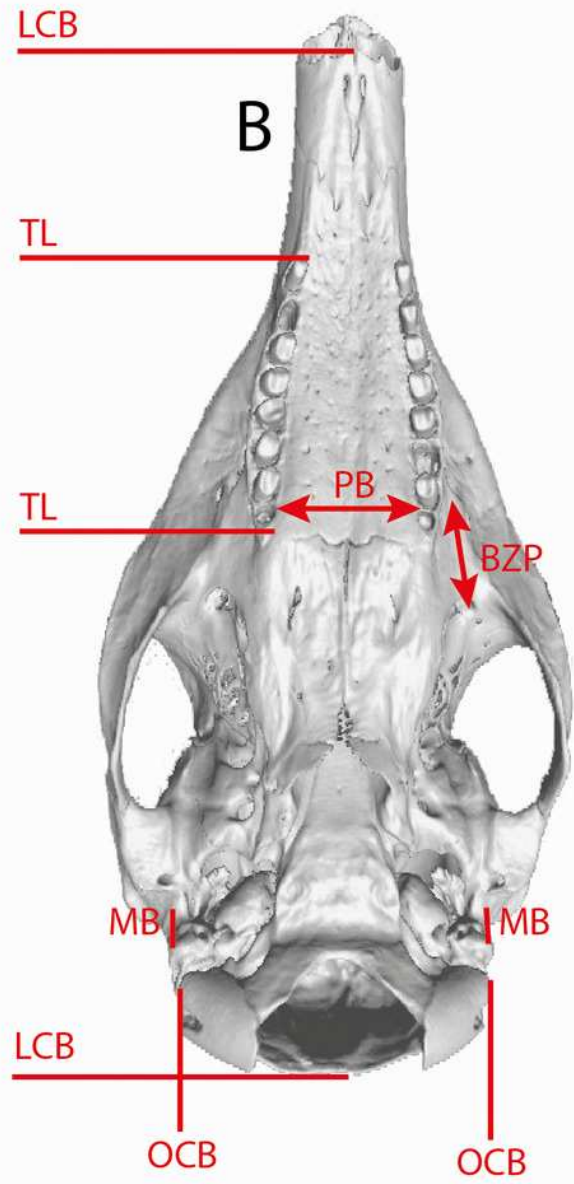
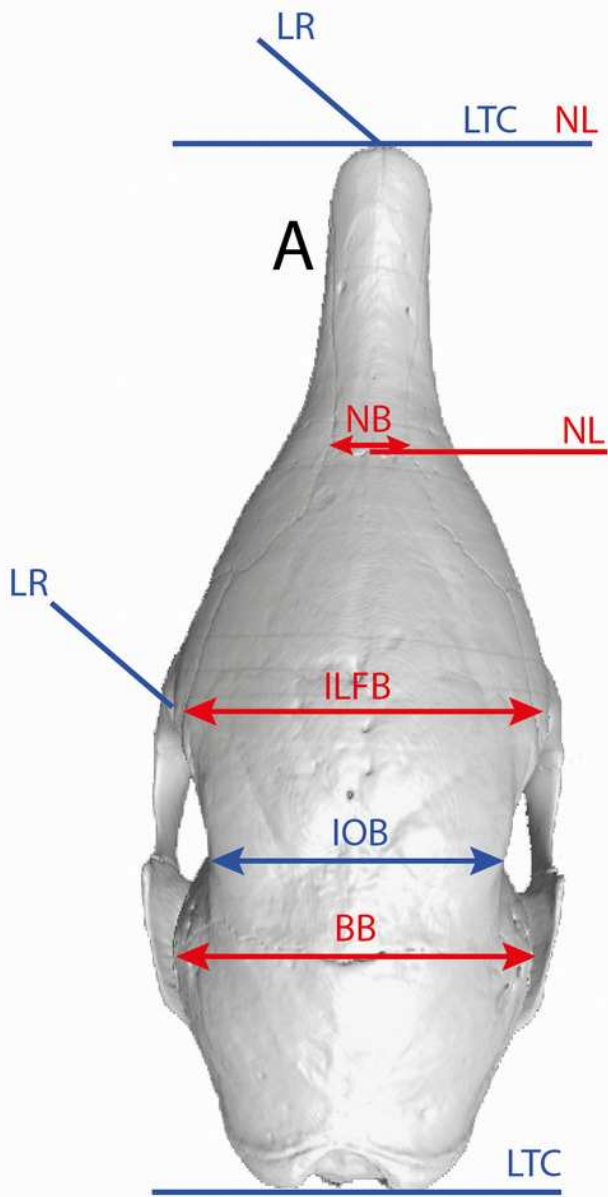


Figure 3

Figure 3

(A) Principal component analysis (PC1 vs PC2) and associate patterns of morphological transformation for the mandible of five *Dasypus* species. (B) Regression of the first principal component on the logarithm of the centroid size ($R^2=0.23$; $p<0.001$). Symbols: blue squares, *D. kappleri*; black crosses, *D. novemcinctus*; green triangles, *D. hybridus*; green diamonds, *D. septemcinctus*; red circles, *D. pilosus*.

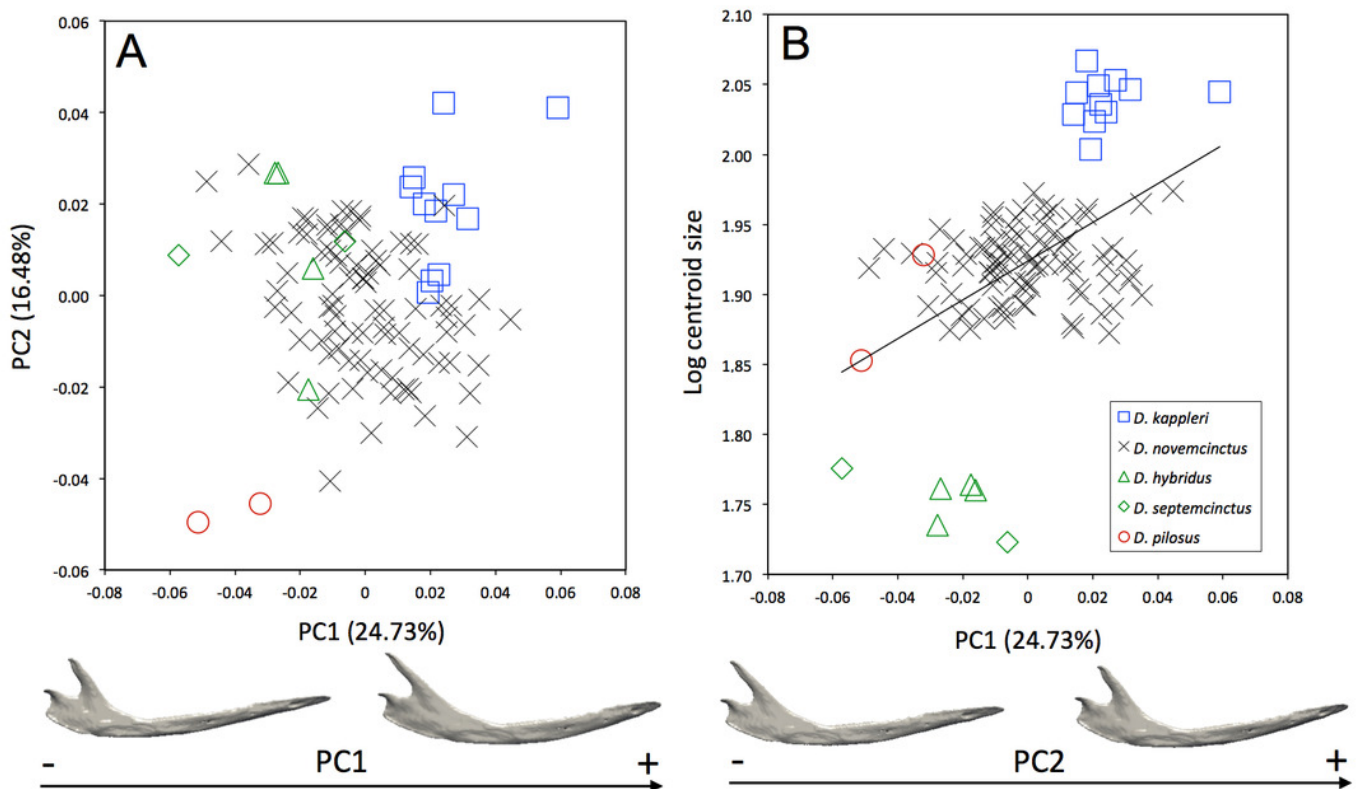


Figure 4

Figure 4

(A) Principal component analysis (PC1 vs PC2) and associate patterns of morphological transformation for crania of five *Dasybus* species. (B) Regression of the first principal component on the logarithm of the centroid size ($R^2=0.55$; $p<0.001$). Symbols: blue squares, *D. kappleri*; black crosses, *D. novemcinctus*; green triangles, *D. hybridus*; green diamonds, *D. septemcinctus*; red circles, *D. pilosus*.

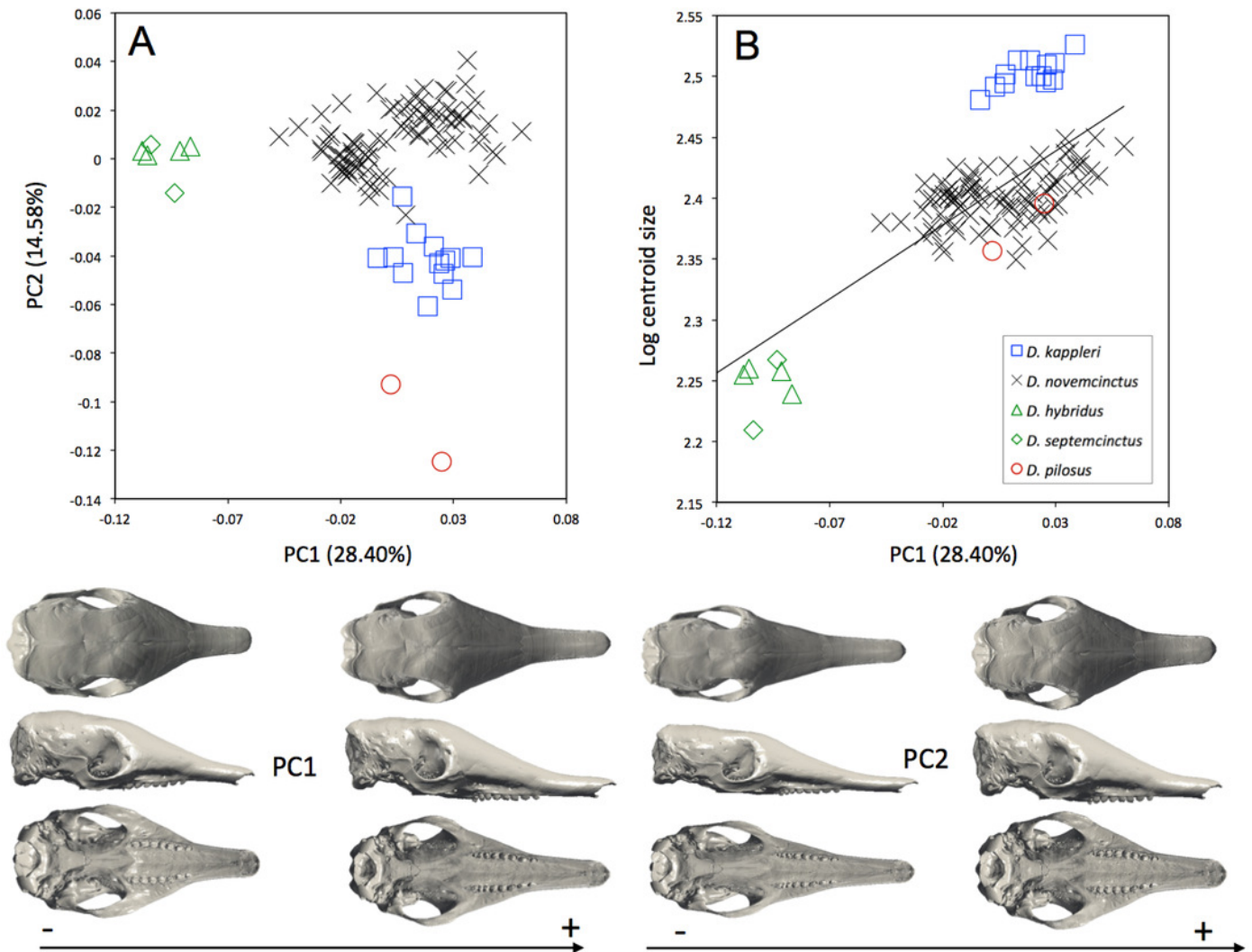


Figure 5

Figure 5

(A) Principal component analysis (PC1 vs PC2) and associate patterns of morphological transformation for mandibles of *Dasypus novemcinctus*. **(B)** Regression of the first principal component on the logarithm of the centroid size ($R^2=0,035$; $p=0.03$). *Symbols:* green diamonds, Bolivia; green triangle, Brazil (solid green triangles are for specimens from Amapa); green circles, Paraguay; green crosses, Peru; green squares, Uruguay; green bars, Venezuela; blue diamonds, Belize; blue “plus”, Guatemala; blue bars, Honduras; Blue squares, Mexico; blue crosses, Nicaragua; blue triangles, USA; blue circles, Costa Rica; black triangles, Colombia; black crosses, Ecuador; black stars, Panama; orange squares, French Guiana; orange crosses, Guyana; orange circles, Suriname.

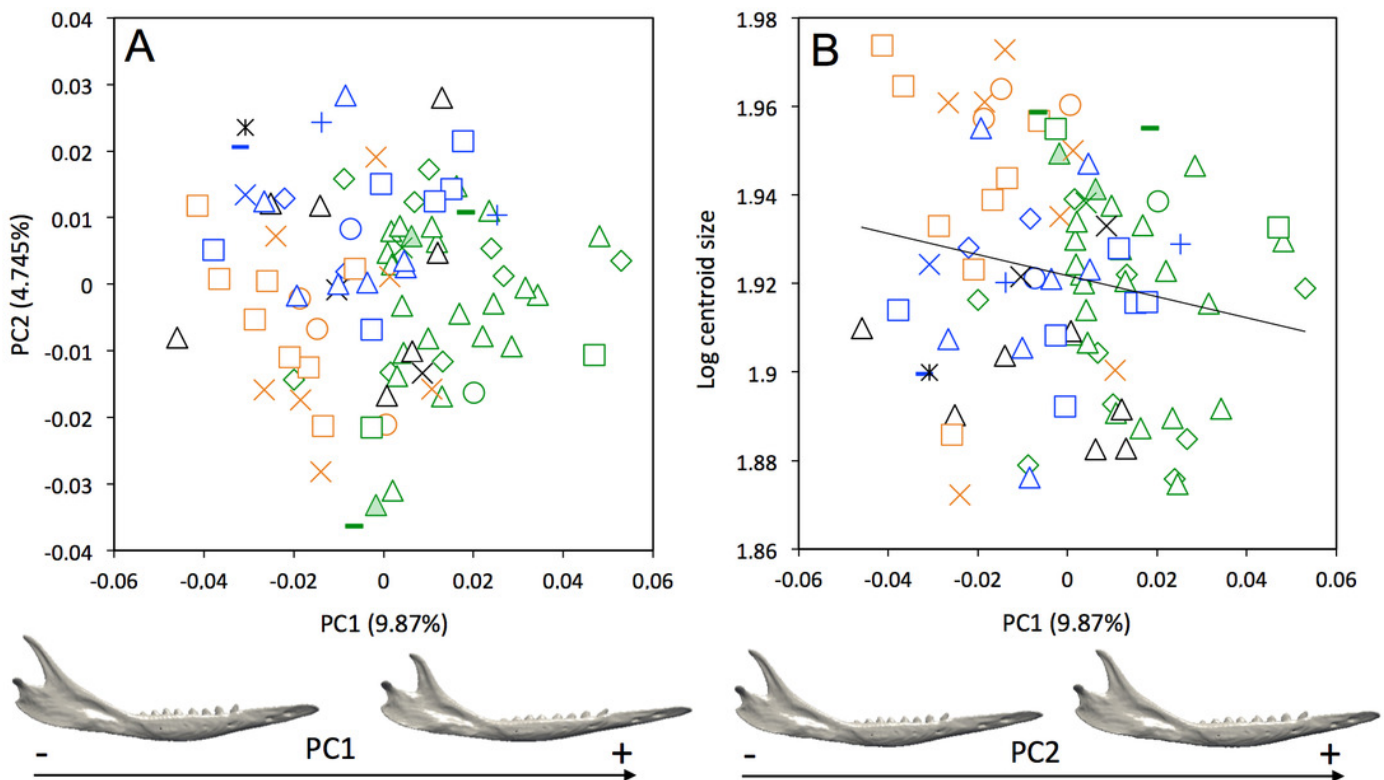


Figure 6

Figure 6

Principal component analysis (**A**, PC1 vs PC2; **B**, PC3 vs PC4) and associate patterns of morphological transformation for crania of *Dasypus novemcinctus*. *Symbols*: green diamonds, Bolivia; green triangle, Brazil (solid green triangles are for specimens from Amapa); green circles, Paraguay; green crosses, Peru; green squares, Uruguay; green bars, Venezuela; blue diamonds, Belize; blue “plus”, Guatemala; blue bars, Honduras; Blue squares, Mexico; blue crosses, Nicaragua; blue triangles, USA; blue circles, Costa Rica; black triangles, Colombia; black crosses, Ecuador; orange squares, French Guiana; orange crosses, Guyana; orange circles, Suriname.

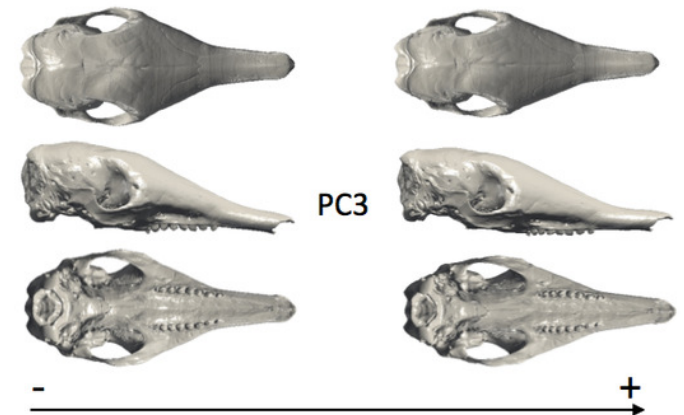
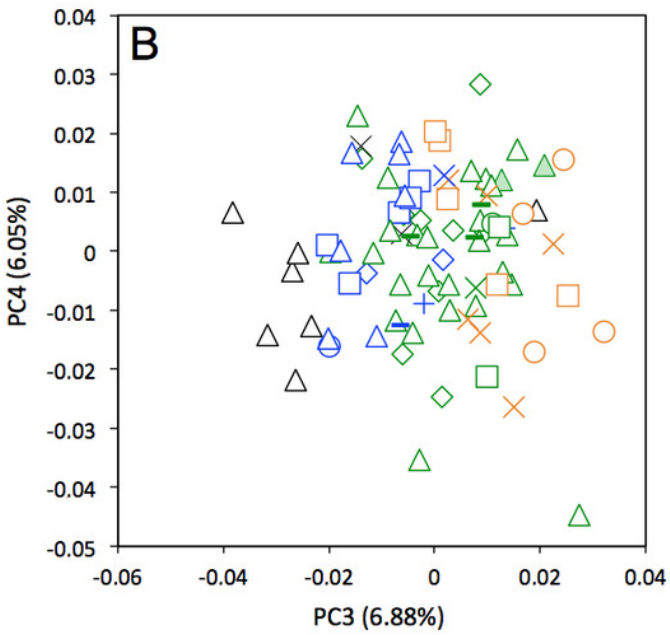
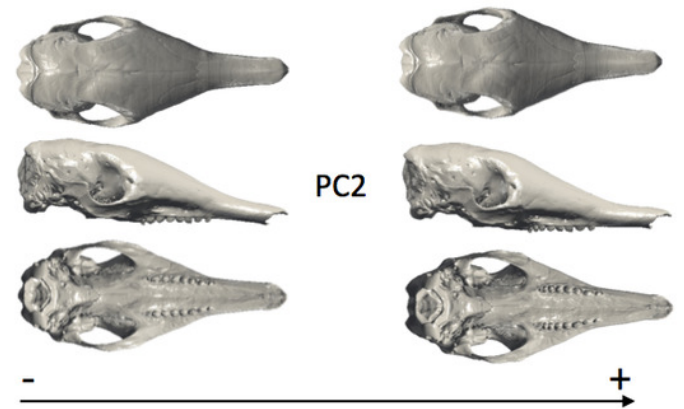
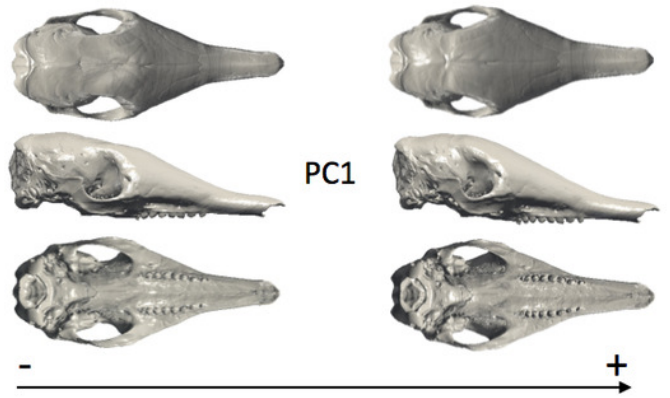
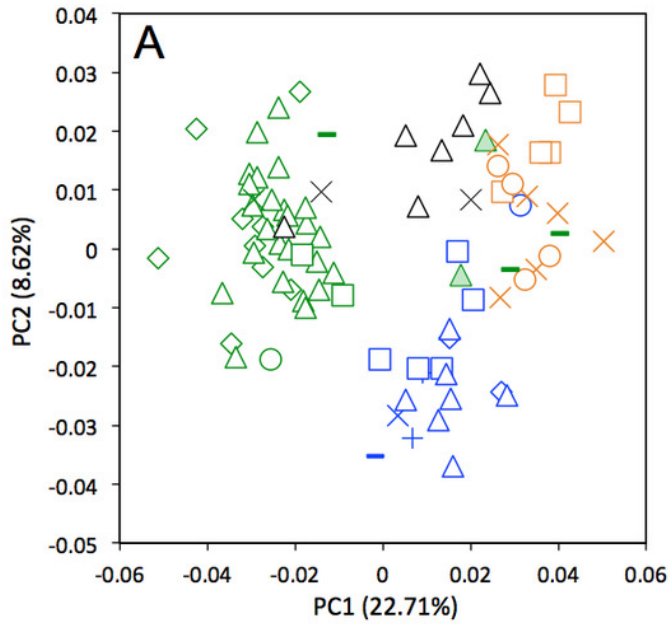


Figure 7

Figure 7

Regression of the first cranial principal component (*Dasypus novemcinctus*) on the logarithm of the centroid size ($R^2=0.15$; $p<0.001$). *Symbols*: green diamonds, Bolivia; green triangle, Brazil (solid green triangles are for specimens from Amapa); green circles, Paraguay; green crosses, Peru; green squares, Uruguay; green bars, Venezuela; blue diamonds, Belize; blue “plus”, Guatemala; blue bars, Honduras; Blue squares, Mexico; blue crosses, Nicaragua; blue triangles, USA; blue circles, Costa Rica; black triangles, Colombia; black crosses, Ecuador; orange squares, French Guiana; orange crosses, Guyana; orange circles, Suriname.

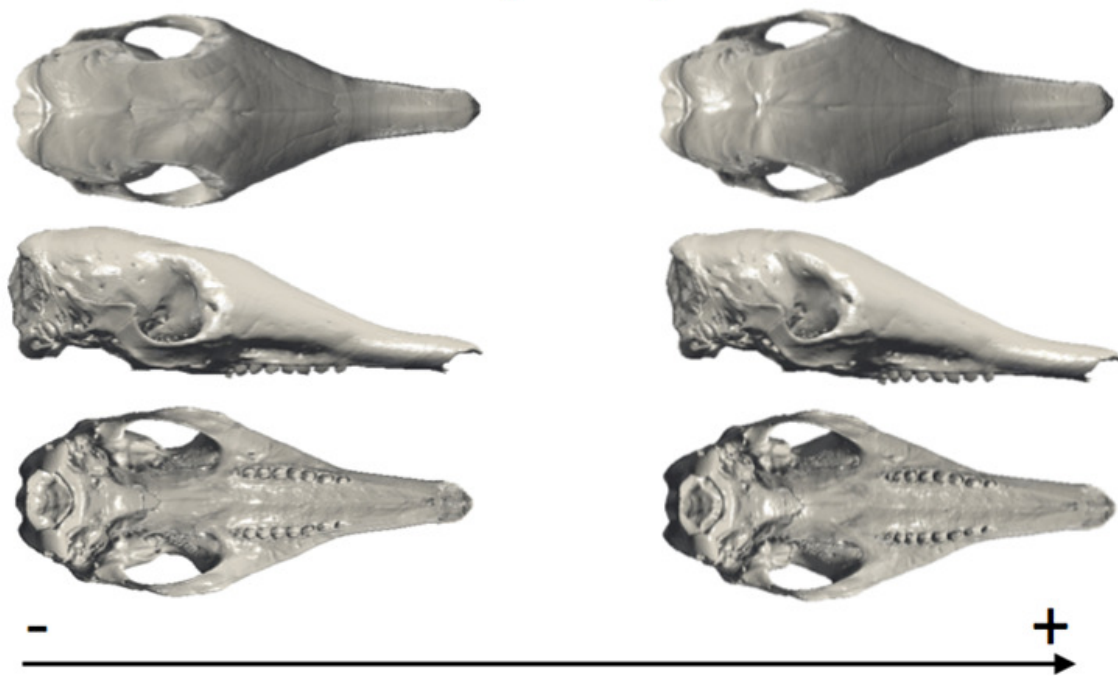
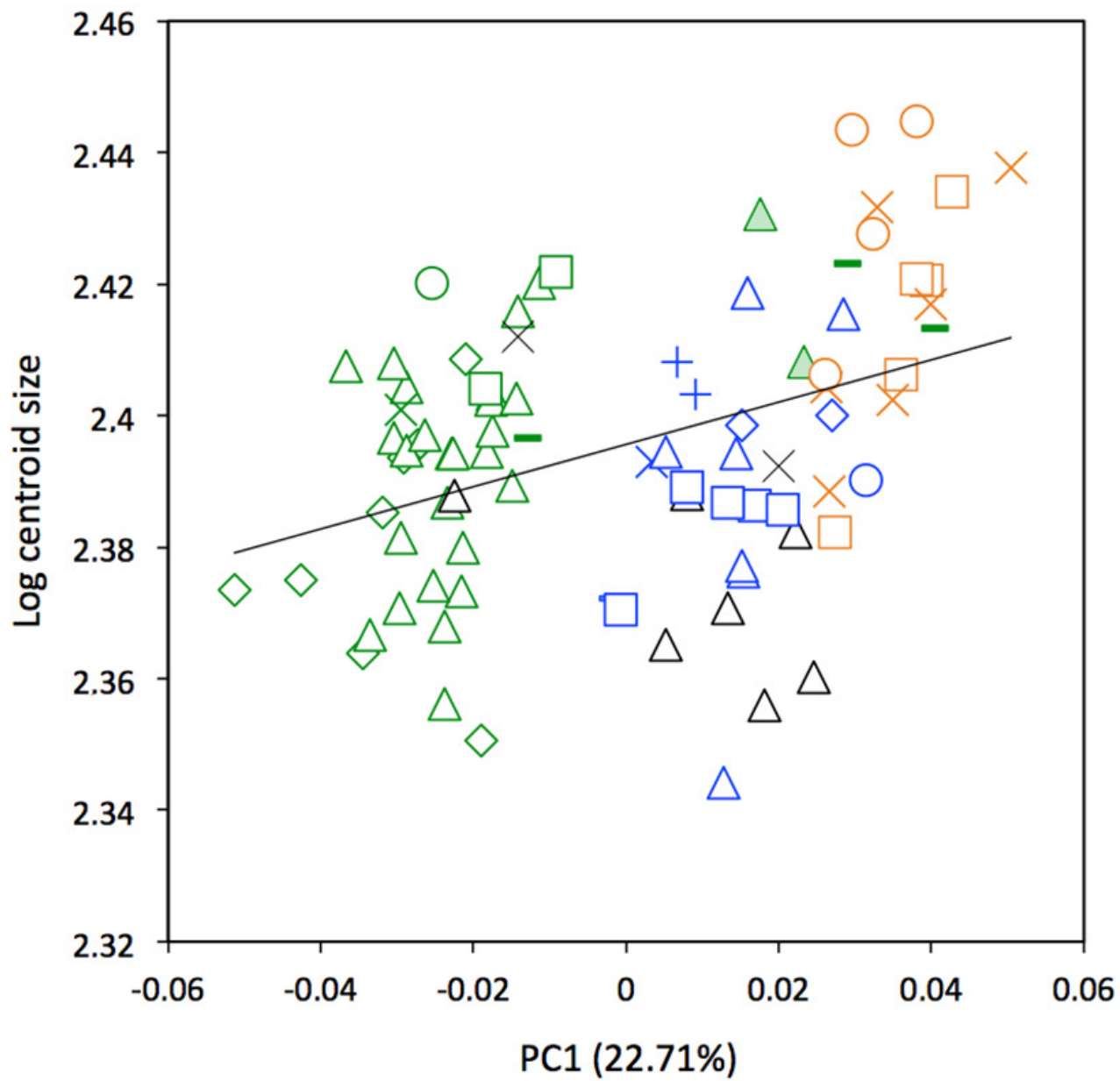


Figure 8

Figure 8

Linear Discriminant Analysis (LDA) performed on cranial shape coordinates of *Dasyops novemcinctus*. Symbols: green diamonds, Bolivia; green triangle, Brazil (solid green triangles are for specimens from Amapa); green circles, Paraguay; green crosses, Peru; green squares, Uruguay; green bars, Venezuela; blue diamonds, Belize; blue “plus”, Guatemala; blue bars, Honduras; Blue squares, Mexico; blue crosses, Nicaragua; blue triangles, USA; black triangles, Colombia; black circles, Costa Rica; black crosses, Ecuador; orange squares, French Guiana; orange crosses, Guyana; orange circles, Suriname.

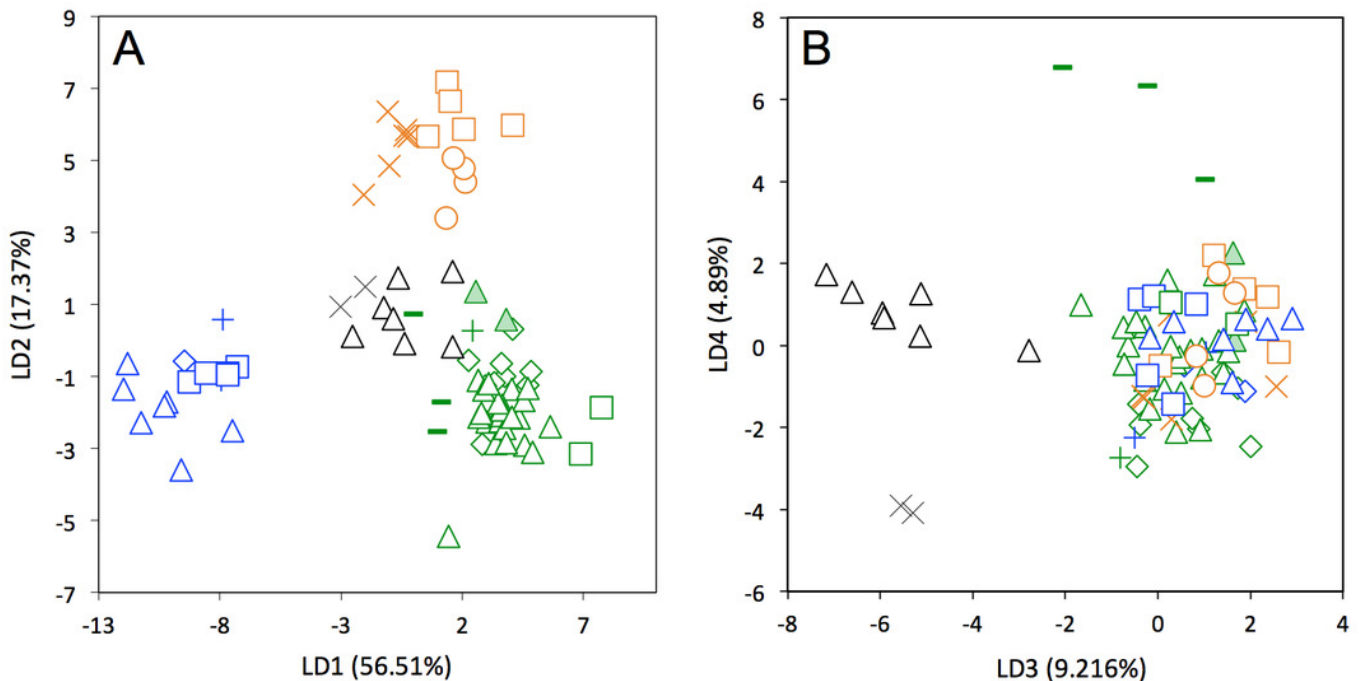


Figure 9

Figure 9

Summary map showing the geographical distribution of nine-banded armadillo specimens investigated in this study and their attribution to one of the four main morphotypes defined in this study: black, Central group; blue, Northern group; green, Southern group; orange, Guianan group. Specimens lacking precise geographical information (other than country of origin) are indicated with a square.

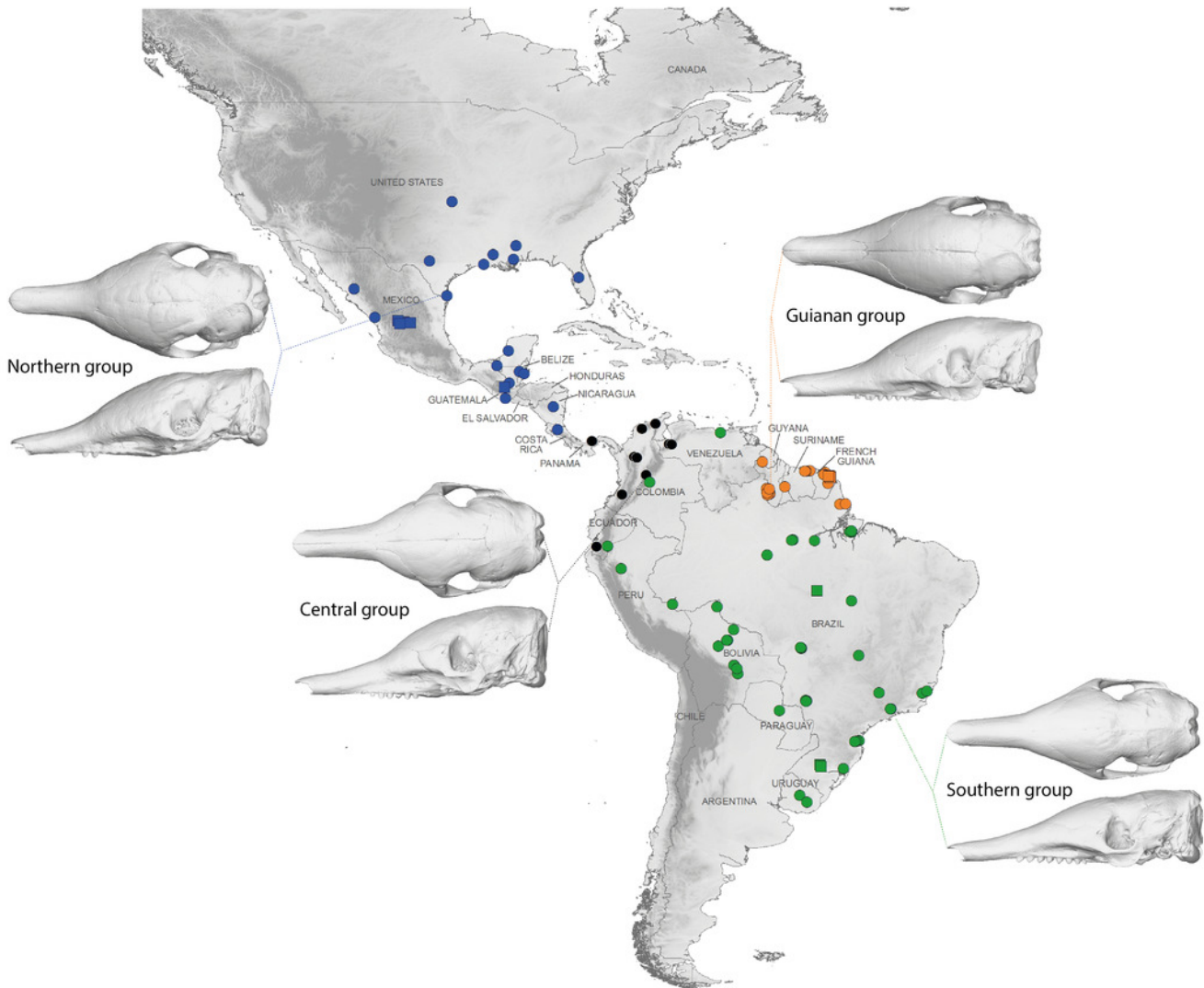


Table 1 (on next page)

Table 1

Definitions of the landmarks used on the mandible

Numbers	Definition
1	Most anterior point of the mandible
2	Most anterior point of the alveolar margin of the tooth row
3	Most posterior point of the seventh tooth
4	Tip of the coronoid process
5	Point at the maximum of concavity between the coronoid and the condyloid processes
6	Most lateral point of the articular surface of the condyle
7	Most medial point of the articular surface of the condyle
8	Point at the maximum of concavity between the condyloid and the angular
9	Tip of the angular process
10	Mandibular foramen

Table 2 (on next page)

Table 2

Definitions of the landmarks used on the cranium. Landmarks indicated with a star were not used in the intraspecific comparisons.

Numbers	Definition
1	Most anterodorsal point of the nasal suture
2	Intersection between inter-nasal and inter-frontal sutures
3	Intersection between inter-parietal and inter-frontal sutures
4	Intersection between inter-parietal and supra-occipital
5	Most distal point of the supra-occipital
6 and 7	Intersection between frontal, maxillar, and nasal sutures
8 and 9	Most dorsomedial point of the orbit (i.e. minimal interorbital length)
10 and 11	Most posterolateral point of the supra-occipital
12 and 28	Most anterolateral point of the premaxillar/nasal suture
13 and 29	Intersection between premaxillar, maxillar, and nasal sutures
14 and 30	Intersection between the lacrimal, maxillar, and frontal sutures
15 and 31	Anteroventral margin of the lacrimal foramen
16 and 32	Anteroventral margin of the upper ethmoid foramen
17 and 33	Most anterior point of the squamosal, frontal, and alisphenoid sutures
18 and 34	Most dorsal point of the maxillary foramen
19 and 35	Most dorsal point of the infraorbital foramen
20 and 36	Most anteroventral point of the sphenopalatine fissure
21 and 37	Most dorsal point of the jugal/maxillar suture
22 and 38	Most dorsal point of the jugal/squamosal suture
23 and 39	Most posterior point of the postglenoid process
24 and 40	Most posterodorsal point of the zygomatic part of the squamosal
25 and 41	Intersection between the frontal, squamosal, and parietal sutures
26 and 42	Most dorsal point of sulcus for external acoustic meatus on squamosal
27 and 43	Intersection between the parietal, squamosal, and supraoccipital sutures
44 and 60	Most posterior point of the premaxillar/maxillar suture in ventral view
45 and 61	Most anterior point of the alveolar margin of the tooth row
46 and 62	Most posterior point of the alveolus of the seventh dental locus
47 and 63	Intersection between the lacrimal/maxillar suture and the zygomasseteric crest in ventral view
48	Intersection between maxillar and palatine sutures
49 and 64	Most posterolateral point of the pterygoid wings
50 and 65	Transverse canal foramen
51 and 66	Most anterodorsal point of the <i>foramen ovale</i>
52 and 67	Most ventral of the alisphenoid/squamosal suture
53 and 68	Most lateral point between the basioccipital/basisphenoid sutures
54 and 69	Most posterolateral point of the jugular foramen
55 and 70	Most posterolateral point of the hypoglossal foramen
56 and 71	Most anterolateral point of the occipital condyle
57 and 72	Intersection between the basioccipital, the occipital condyle, and the <i>foramen magnum</i>
58	Most antero-ventral point of the <i>foramen magnum</i>
59	Most postero-dorsal point of the <i>foramen magnum</i>
73 and 74	Intersection between the supraoccipital, exoccipital, and petrosal sutures
75 and 76	Most posterior point of the postglenoid foramen
77 and 78	Caudal palatine foramen
79* and 80*	Point of maximum concavity on the maxillar/frontal suture in dorsal view
81 and 82	Intersection between the lacrimal/frontal suture and the orbit
83	Most posterior point of the frontal sinuses in the midline
84	Ventral tip of the tentorial process